

Copyright
by
Emily Megan Graham

2011

**The Thesis Committee for Emily Megan Graham
Certifies that this is the approved version of the following thesis:**

**Three-dimensional gas migration and gas hydrate systems of south
Hydrate Ridge, offshore Oregon**

**APPROVED BY
SUPERVISING COMMITTEE:**

Supervisor:

Nathan L. Bangs

Peter Flemings

Robert Tatham

**Three-dimensional gas migration and gas hydrate systems of south
Hydrate Ridge, offshore Oregon**

by

Emily Megan Graham, B.S.

Thesis

Presented to the Faculty of the Graduate School of
The University of Texas at Austin
in Partial Fulfillment
of the Requirements
for the Degree of

Master of Science in Geological Sciences

The University of Texas at Austin

May 2011

Acknowledgements

I'd like to thank my supervisor, Dr. Nathan Bangs for the opportunity to work on this research as well as the mentoring he provided throughout my time at the University of Texas at Austin. I'd also like to thank my committee members, Dr. Robert Tatham and Dr. Peter Flemings, for their helpful suggestions and edits. I'm thankful to the Jackson School of Geosciences, the University of Texas Institute for Geophysics, and the Society for Exploration Geophysicists for providing funding throughout my education and research career.

May 2011

Abstract

Three-dimensional gas migration and gas hydrate systems of south Hydrate Ridge, offshore Oregon

Emily Megan Graham, M.S. Geo. Sci.

The University of Texas at Austin, 2011

Supervisor: Nathan L. Bangs

Hydrate Ridge is a peanut shape bathymetric high located about 80 km west of Newport, Oregon on the Pacific continental margin, within the Cascadia subduction zone's accretionary wedge. The ridge's two topographic highs (S. and N. Hydrate Ridge) are characterized by gas vents and seeps that were observed with previous ODP initiatives. In 2008, we acquired a 3D seismic reflection data set using the P-Cable acquisition system to characterize the subsurface fluid migration pathways that feed the seafloor vent at S. Hydrate Ridge.

The new high-resolution data reveal a complex 3D structure of localized faulting within the gas hydrate stability zone (GHSZ). We interpret two groups of fault-related migration pathways. The first group is defined by regularly- and widely-spaced (100-150 m) faults that extend greater than 300ms TWT (~ 250 m) below seafloor and coincide with the regional thrust fault orientations of the Oregon margin. The deep extent of these faults makes them potential conduits for deeply sourced methane and may include

thermogenic methane, which was found with shallow drilling during ODP Leg 204. As a fluid pathway these faults may complement the previously identified sand-rich, gas-filled stratigraphic horizon, Horizon A, which is a major gas migration pathway to the summit of S. Hydrate Ridge. The second group of faults is characterized by irregularly but closely spaced (~ 50 m), shallow fractures (extending < 160 ms TWT below seafloor, ~ 115 m) found almost exclusively in the GHSZ directly beneath the seafloor vent at the summit of S. Hydrate Ridge. These faults form a closely-spaced network of fractures that provide multiple migration pathways for free gas entering the GHSZ to migrate vertically to the seafloor. We speculate that the faults are the product of hydraulic fracturing due to near-lithostatic gas pressures at the base of the GHSZ. These fractures may fill with hydrate and develop a lower permeability, which will lead to a buildup of gas pressures below the GHSZ. This may lead to a vertical propagation of new fractures to release the overpressure, which results in the high concentration of shallow fractures within the GHSZ seen in the 2008 data.

Table of Contents

List of Figures	ix
Chapter 1: Introduction	1
Methane Hydrates	1
Methane Generation & Natural Hydraulic Fracturing	8
South Hydrate Ridge Geological Setting	10
Objectives	22
Chapter 2: 3D Seismic Reflection Data	23
Seismic Acquisition	23
<i>P-Cable System</i>	24
<i>Acquisition Parameters</i>	25
Seismic Data Processing	27
Interpretation Strategies & Observations	33
Chapter 3: Gas Supply System	41
Methane Origin	41
Horizon A	43
Discussion	47
Conclusions	48
Chapter 4: Venting Processes and Hydrate Formation	50
Faults	50
Natural Hydraulic Fracturing & Hydrate Formation	56
Discussion	62
Conclusions	65
Chapter 5: South Hydrate Ridge Migration System Discussion	67
Fracture Development	67
Reflection Amplitude Analysis	72

Chapter 6: Summary	77
References	80
Vita	87

List of Figures

- Figure 1: Global Gas Hydrate Locations. Red circles indicate marine gas hydrates and diamonds indicate permafrost hydrates. Hydrate specific drill sites prior to 2002 are also listed (Collett, 2002. AAPG©2002 reprinted by permission of the AAPG whose permission is required for further use).
.....3
- Figure 2: Pressure-temperature graph with respect to depth. The lines plotted represent conditions under which methane will form into gas hydrate with varying water and methane chemistry. Labels on the graph show examples from drill sites on Blake Ridge, the Cascadian margin, and the Chilean Triple Junction (reprinted with permission from Rao et al., 2001).5
- Figure 3: Examples of gas hydrate recovered from Hydrate Ridge during Ocean Drilling Program Leg 204. A and B depict samples from hydrate mounds recovered near the seafloor, while C and D are massive hydrates sampled from the upper 30mbsf (reprinted with permission from Torres et al., 2004).6
- Figure 4: Example of a Bottom Simulating Reflection (BSR) at Blake Ridge, offshore South Carolina, on a 2D seismic reflection line, with the zone of hydrate formation (GHSZ) labeled (Modified from Shipley et al., 1979).7
- Figure 5: Model of micro-cracks within a medium connecting to form a fracture network (Modified with permission from Luo and Vasseur, 2002). ..9

Figure 6: (A) Hydrate Ridge, located on the Cascadia accretionary margin (reprinted with permission from Torres et al., 2004) (B) drill sites from ODP Leg 204 as black circles and the approximate 3D seismic survey area shot in 2000 in red. (C) Zoomed in map of the ODP Leg 204 drill sites.12

Figure 7: Previous seismic reflection profiles across south Hydrate Ridge (reprinted with permission from Tréhu et al., 2006).A) Regional profile OR89_line2 from ODP Leg 146 (originally from MacKay et al., 1992) showing the offshore Oregon accretionary complex. B) Interpreted seismic section from A converted into depth. C) Seismic slice from 3D survey acquired in 2000 that coincides with box in A (Tréhu et al., 2006).13

Figure 8: Tectonic evolution of south Hydrate Ridge based on the 2000 data, which is responsible for uplifting the deep-sea fan complexes (reprinted with permission from Chevallier et al., 2006).14

Figure 9: (left) The summit of south Hydrate Ridge is characterized by an authigenic carbonate pinnacle and seafloor gas seeps, approximate seep area shown in green. (right) An acoustic image (modified from Heeschen et al., 2003) of free gas venting from the summit of south Hydrate Ridge, with an approximate line location shown in red.16

Figure 10: Hydrate concentrations (colored overlays) at south Hydrate Ridge from the 2000 3D reflection volume. The map represents hydrate concentration averaged from the seafloor to the BSR. The anomalously bright Horizon A is also apparent on B, C, D, and E cross sections (reprinted with permission from Tréhu et al., 2006).....	18
Figure 11: A) LWD in situ bulk density and grain size distribution at site 1245, showing anomalous Horizon A at ~175mbsf (reprinted with permission from Tréhu et al., 2004b). B) C_1/C_2 ratio and isotopic composition of methane at sites 1245 and 1247, showing low C_1/C_2 and high isotopic composition at Horizon A, indicating migrated gas. Gas chemistry within the GHSZ is indicative of biogenic gas (reprinted with permission from Tréhu et al., 2006). C) Chemistry of methane at the summit, indicating migrated gas in Horizon A and the upper 20-30mbsf. (reprinted with permission from Tréhu et al., 2006).....	19
Figure 12: Amplitudes of Horizon A extracted from the 2000 data volume, showing the gas-water contact in dashed green and the BSR and Horizon A intersection in dashed yellow (reprinted with permission from Tréhu et al., 2004b).	20
Figure 13: Gas pressure at site 1250 and gas effective stress mapped along south Hydrate Ridge's summit (reprinted with permission from Tréhu et al., 2004b).	21

Figure 14: Survey area for the south Hydrate Ridge 2008 3D seismic reflection volume (regional inset reprinted with permission from Torres et al., 2004).	23
Figure 15: P-Cable set up, utilizing 10 single-channel streamers, which was used to acquire the 2008 3D seismic volume.	25
Figure 16: HR3D08 data frequency in amplitudes scaled to decibels (top) and linear scaling (bottom).	26
Figure 17: Fold map displaying the survey's data coverage. On average the bins contained between 4 (blue) and 8 fold (green), with a maximum of 18 (red).	28
Figure 18: Noise reduction comparisons on (a) a single shot gather using (b) a de-spiking tool and (c) a trapezoidal bandpass filter (1,25,180,250).	29
Figure 19: Noise reduction comparisons on (a) a stacked inline using (b) a de-spiking tool and (c) a trapezoidal bandpass filter (1,25,180,250).	30
Figure 20: (Left) Migrated stack of crossline 210, using a Kirchhoff post-stack 3D migration with a velocity model of 1500m/s (Right) Un-migrated stack of crossline 210. Red arrows designate examples of reflections enhanced through migration.	32
Figure 21: Crossline 600 showing a prominent, continuous bright amplitude reflection beneath the seafloor (shown by arrow) and loss of signal beneath ~1.4s.	34

Figure 22: A cut-away 3D cube view showing a prominent, continuous bright amplitude reflection of the seafloor and the BSR beneath the seafloor.	35
Figure 23: Depth map in msbsl of BSR (contour interval of 30ms).	36
Figure 24: Crossline 557, depicting multiple, non-continuous reflections that vary laterally in amplitude and a blank-out zone of dim amplitudes.	36
Figure 25: Inline 260 showing an anomalously bright amplitude north-dipping reflection imaged below the BSR called Horizon A.	37
Figure 26: Depth map in msbsl of Horizon A (contour interval of 20ms).	37
Figure 27: Instantaneous amplitudes of BSR (left) and Horizon A (right) with the seafloor contour overlay (50ms interval) in white. Note the incidences of high amplitudes (shown by white arrows) along the BSR on the eastern flank of the ridge and those on Horizon A, at the summit and on the northern flank.	39
Figure 28: Gas saturation (S_g) for ODP sites 1245, 1247, 1248, and 1250 calculated by Tréhu et al. (2004b) using LWD bulk density logs and average porosity and density from moisture and density measurements. The depths of the observed high gas saturations correspond with the seismically imaged Horizon A (reprinted with permission from Tréhu et al., 2004b).	42

Figure 29: Bulk Density (A) and grain size (B) for Site 1245, with moisture and density measurements for Horizon A (C) and core image showing ash-rich layers of Horizon A (D) (reprinted with permission from Tréhu et al., 2004b).	44
Figure 30: Crossline 584, with an arrow showing Horizon A entering the GHSZ (the base of which is the BSR) directly beneath the carbonate pinnacle.	46
Figure 31: Examples of vertical and horizontal discontinuities along crossline 915.	51
Figure 32: 3D view of vertically lined displacements.	53
Figure 33: Crossline 915, example of a selection of interpreted thrust faults.	53
Figure 34: Example of vertically lined displacements, interpreted as a thrust fault in 3D cube view.	54
Figure 35: Map of the major interpreted thrust faults which are primarily located on the flanks of south Hydrate Ridge. The three northern most faults may play a role in supplying deeply sourced thermogenic methane to the system.	55
Figure 36: Example of an uninterpreted fracture (pink fracture) in a 3D cube volume	58
Figure 37: Example of the interpreted pink fracture network in a 3D cube view.	59
Figure 38: Clipped perspective view, looking South, of a selection of summit fractures, with each color corresponding to an individual fracture. 9 of the fractures shown terminate at or just below the BSR, while only 6 penetrate Horizon A.	60

Figure 39: Zoomed-in view of the interpreted fracture networks located along the summit of south Hydrate Ridge.	61
Figure 40: (left) Gamma density measurements and X-ray image of 4inch core from offshore India where hydrate was imaged within vertical fractures. (center) X-ray image of core from offshore India where gas hydrate nodes were imaged as well as gas hydrate within vertical fractures (right) P-wave velocity, gamma density and X-ray image of core sampled from offshore India. Notice the network of vertical, hydrate-filled fractures imaged by the core X-ray (modified from Collett, 2006).	64
Figure 41: Fluid migration and fracture development process.	71
Figure 42: Clipped perspective view of a selection of summit fractures (looking south) with each color corresponding to an individual fracture. The fractures which penetrate Horizon A correspond to incidents of high amplitudes.	74
Figure 43: Map view of the fractures that penetrate Horizon A with respect to Horizon A's instantaneous amplitudes. Note how the blue, lime green and pink fractures bound the zone of highest amplitude where the greatest concentration of gas is assumed to be.	75
Figure 44: Perspective view looking up-dip of Horizon A (south). Fractures that penetrate Horizon A are shown with respect to Horizon A's instantaneous amplitude. The blue, lime green and pink fracture systems bound the bright amplitude zone where gas is assumed to be.	76

Chapter 1: Introduction

Gas hydrates and the conditions in which they form are well understood, however the intricate internal processes occurring within the gas hydrate stability zone are less so. The objective of this thesis is to examine the plumbing system that provides, migrates, and vents the methane needed for gas hydrate growth at south Hydrate Ridge, offshore Oregon. Hydrate Ridge is an active research site with studies focusing on hydrate development, geochemical reactions, and active seafloor venting and microbial communities. The well constrained physical, thermal and chemical processes occurring at south Hydrate Ridge make it an excellent environment for studying the interaction between gas migration and gas hydrate formation. Understanding the nature of how free gas interacts with a gas hydrate environment could help further research on shallow hazards, hydrate economics and global methane impact. I believe natural fractures play an important role in south Hydrate Ridge's fluid migration and venting system, and may be created by over-pressurized gas at south Hydrate Ridge. This thesis will examine the role of highly pressurized gas in the formation of natural fractures and the fractures' control on methane venting at the summit of south Hydrate Ridge.

METHANE HYDRATES

South Hydrate Ridge is characterized by accumulations of gas hydrates within the subsurface and on the seafloor. Gas hydrates form when water molecules encase a gas molecule in a cage-like lattice structure of ice. Frequently observed guest molecules include ethane, propane, butane, carbon dioxide, hydrogen sulfide, and methane (Sloan, 1998). Although multiple gases can form into hydrate, methane comprises over 99% of natural gas hydrate (Kvenvolden and Lorenson, 2001). Due to the volatile nature of their

guest gas molecules, hydrate studies focus on a multitude of economic, energy, and climate change issues over the last decade (Kvenvolden, 1998; Henriot and Mienert, 1998; Judd, 2003; and Walsh et al., 2009). The Cascadia margin in particular is the focus of studies evaluating the viability of producing gas hydrate as an energy source due to the high concentration of massive hydrate accumulations (Collett and Kuuskraa, 1998). The commerciality of producing energy from hydrate and the effects hydrates have on the global carbon cycle are important because a single m^3 of methane hydrate can contain up to 163m^3 of free methane gas at atmospheric pressure (Kvenvolden, 1998). The high concentration of gas within hydrates yielded conservative worldwide estimates of 676,000tcf (trillion cubic feet) of natural gas trapped in hydrate, which is significant when compared to the estimated 6,000tcf of recoverable natural gas worldwide (Collett and Kuuskraa, 1998; and Johnson 2006).

The global distribution of natural hydrates, with hydrates speculated in every tectonic setting and ocean, is another cause for their increasing scientific and economic interest. In the United States, the three major areas of gas hydrate interest are the Blake Ridge of offshore South Carolina, the Gulf of Mexico Basin Province, and the Cascadia margin. Worldwide, major hydrate rich regions include northern Russia, the Alaskan North Slope, the Black Sea, the Caspian Sea, the Sea of Okhotsk, offshore Peru, and the Japan eastern and western margins (Collett & Kuuskraa, 1998). Figure 1 displays locations of known and inferred gas hydrate accumulations and the sites of hydrate-specific drilling initiatives prior to 2002. The known marine hydrate locations are identified through deep sea drilling initiatives and seafloor sampling, while the remaining locations are inferred through seismic identification of a bottom-simulating-reflection, the “BSR”. The Ocean Drilling Program (ODP) and International Ocean Drilling Program

(IODP) dedicated specific studies to recovering cored gas hydrate from Blake Ridge and Hydrate Ridge, on the Cascadia margin. Gas hydrate presence was often only inferred in recovered cores and rarely directly observed prior to the drilling on Blake Ridge and Hydrate Ridge (Collett, 2002).

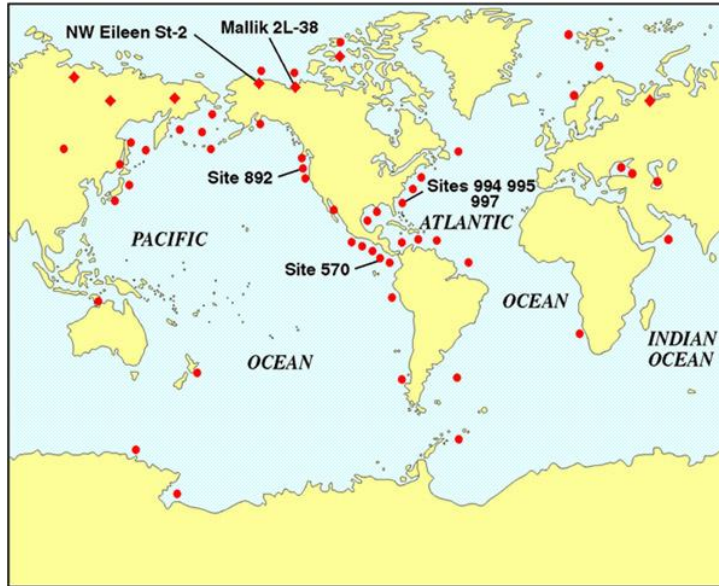


Figure 1: Global Gas Hydrate Locations. Red circles indicate marine gas hydrates and diamonds indicate permafrost hydrates. Hydrate specific drill sites prior to 2002 are also listed (Collett, 2002. AAPG©2002 reprinted by permission of the AAPG whose permission is required for further use).

The well constrained temperature and pressure conditions under which methane forms into hydrate makes inferring worldwide locations of gas hydrate possible. These conditions are met in low temperatures and high pressure environments, such as arctic permafrost and shallow (300-500m water depths) seafloor sediments where temperatures approach 0°C (figure 2). The geothermal gradient determines the depths to which hydrates can form, with a maximum of roughly 2000m below the seafloor (Kvendolden and Lorenson, 2001). Gas hydrates can form as structural accumulations, stratigraphic

accumulations, or a combination of both structural and stratigraphic (Milkov and Sassen, 2002). In the structural case, methane travels along faults or mud volcanoes and accumulates as large, densely filled veins or layers. These are commonly massive deposits (centimeters and greater in size) (Milkov and Sassen, 2002). Figure 3 is an example of massive hydrates recovered from mounds on the seafloor (A and B) and recovered from sediments 30m below the seafloor (C and D) of south Hydrate Ridge. In a stratigraphic accumulation, the gas hydrate is trapped within the pore space of a permeable layer and is often widely dispersed in low concentrations (millimeters and less in size) (Milkov and Sassen, 2002). The massive hydrate nodes and mounds recovered from south Hydrate Ridge are evidence of a porous and permeable subsurface, with large amounts of methane entering the system.

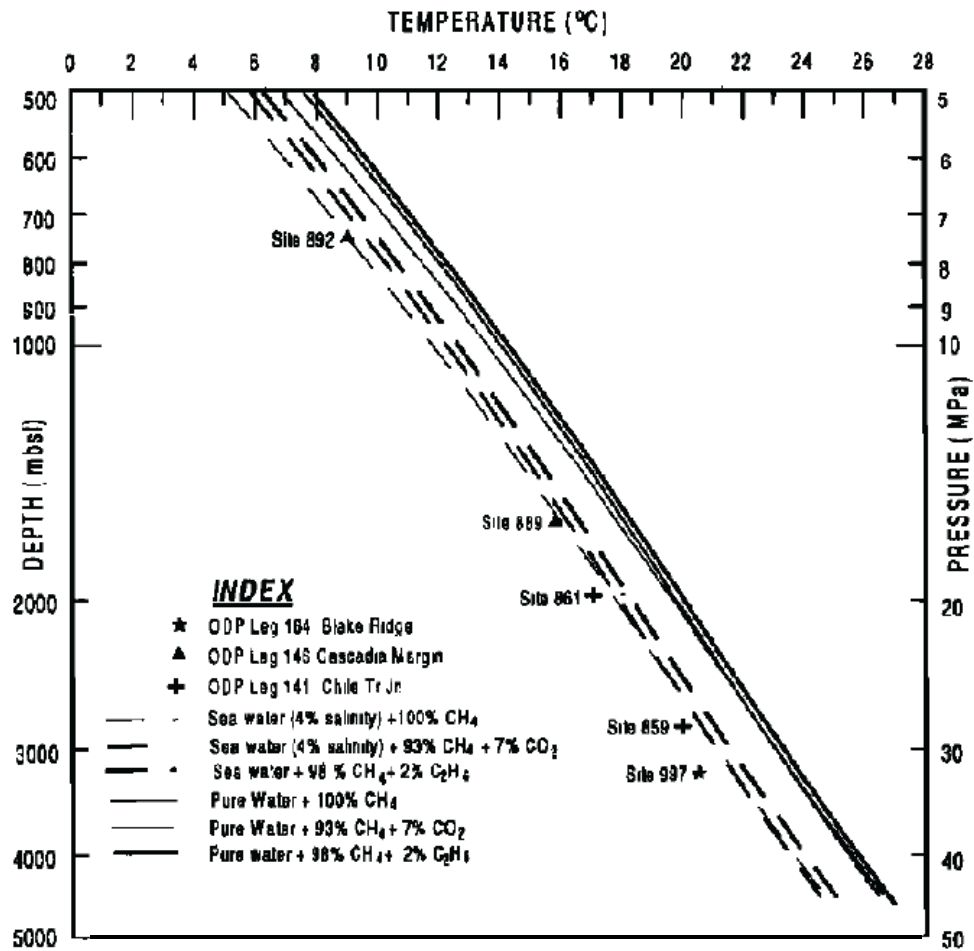


Figure 2: Pressure-temperature graph with respect to depth. The lines plotted represent conditions under which methane will form into gas hydrate with varying water and methane chemistry. Labels on the graph show examples from drill sites on Blake Ridge, the Cascadian margin, and the Chilean Triple Junction (reprinted with permission from Rao et al., 2001).

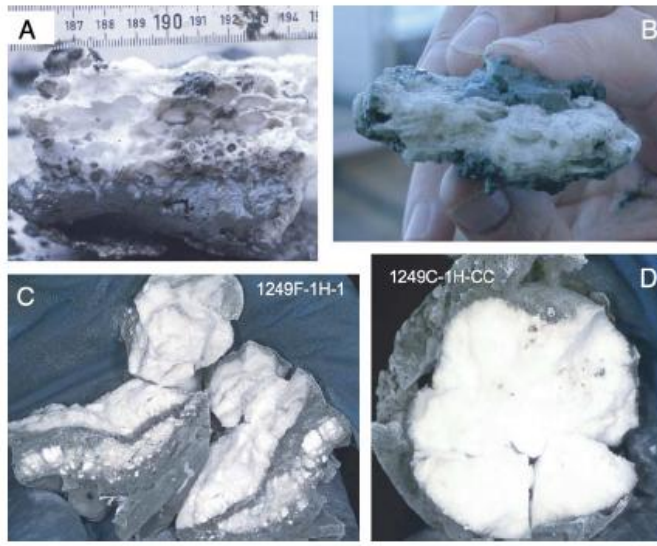


Figure 3: Examples of gas hydrate recovered from Hydrate Ridge during Ocean Drilling Program Leg 204. A and B depict samples from hydrate mounds recovered near the seafloor, while C and D are massive hydrates sampled from the upper 30mbsf (reprinted with permission from Torres et al., 2004).

The gas hydrate stability zone, here-after referred to as the GHSZ, is the subsurface area where conditions favor gas hydrate formation and is identifiable in marine seismic reflection data. The base of the GHSZ is a thermobaric (temperature and pressure) boundary between hydrate deposits and possibly dissolved or free gas. Hydrate presence in marine sediment causes an increase in sediment velocity and a slight decrease in sediment density (MacKay et al., 1994). Small accumulations of free gas in sediments result in a drastic decrease in seismic wave velocity. Therefore, the sonic velocity is higher in the hydrate zone and significantly decreases as it travels out of the GHSZ and into the free gas accumulations. The resulting change in acoustic impedance produces an anomalously bright, negative amplitude reflection that mimics the sea floor with opposite reflection polarity and crosscuts the surrounding geology, known as a bottom-simulating-reflection or “BSR” (figure 4). The origin of BSRs is debated between a result of the

presence of low velocity free gas beneath the GHSZ (MacKay et al., 1994; Bangs et al., 1993; and Singh et al., 1993), a result of the high velocity hydrate above non-hydrate sediment (Hyndman and Davis, 1992), or a combination of the two (Miller et al., 1991). Despite its controversial origin, the BSR is used to seismically infer the base of the gas hydrate stability zone where drilling is unavailable (Collett, 2002). Hydrate Ridge has a bright, continuous amplitude BSR beneath the southern and northern ridges, both of which were drilled and gas hydrates were inferred from the sampled cores (Tréhu et al., 2004b; and Milkov et al., 2003).

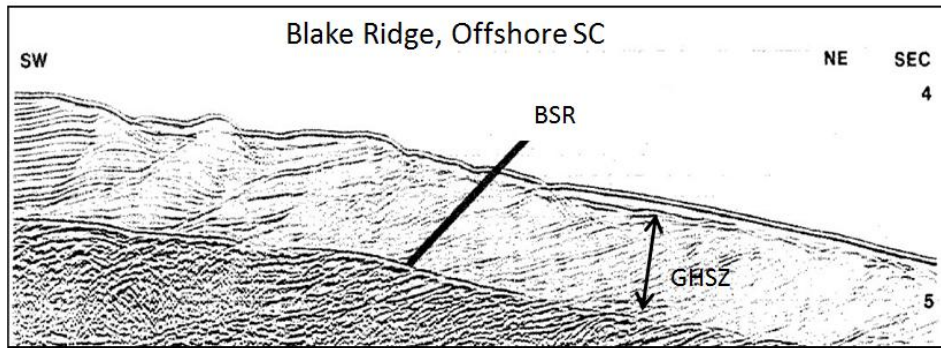


Figure 4: Example of a Bottom Simulating Reflection (BSR) at Blake Ridge, offshore South Carolina, on a 2D seismic reflection line, with the zone of hydrate formation (GHSZ) labeled (Modified from Shipley et al., 1979).

The extensive compaction of gas volume into a hydrate compound and the global distribution of hydrates make gas hydrates a potential energy source, however the economic feasibility of producing gas hydrates is questionable. The locations of gas hydrate reservoirs play a crucial role in evaluating the economic potential of hydrate plays. In countries where foreign dependency on gas is high, such as Japan, the costs of gas hydrate production may be less than importing foreign gas. Also, production of gas hydrate plays will be cheaper if there is a pre-existing oil and gas infrastructure (Walsh et

al., 2009). A major concern with producing gas hydrates is hydrate destabilization, where the sudden release in pressure through drilling would cause the hydrate to revert to free gas and could be responsible for blowouts, mass landslides or slope failures (Suess et al., 1999; and Walsh et al., 2009). Characterizing the fluid migration within a gas hydrate environment may provide insight into avoiding destabilization.

METHANE GENERATION & NATURAL HYDRAULIC FRACTURING

The source of the gas is a critical consideration for the migration and development of vent systems for the methane. Two forms of methane generation occur in marine sediments, biogenic and thermogenic. Biogenic or microbial methane is generated by the decomposition of organic matter in anaerobic conditions by bacteria. This generally occurs under near-surface conditions that support bacterial growth and ceases at greater depths from increases in temperature and rock compaction (Hedberg, 1979). Thermogenic methane is generated by chemical decomposition of organic matter as temperature increases with burial. Typically, thermogenic methane generation is dominant at depths greater than 600m and generation increases with depth (Hedberg, 1979). Methane can migrate to shallower depths along stratigraphic conduits, such as porous and permeable layers, or along structural features, such as faults and fractures.

Development of fractures is a result of over-pressuring in both the fluid phase (hydraulic fracturing) and in the gas phase. Natural hydraulic fracturing occurs when overlying sediments crack to produce fractures as pore-pressure reaches the least principal stress and exceeds the overlying sediment's tensile strength (Hubbert and Willis, 1957; Luo and Vasseur, 2002; and Hustoft et al., 2007). This results in a loss of fluid pressure. Fractures formed by natural hydraulic fracturing are generally elongated

with orientations normal to the least principal stress and have limited lateral extension (Hubbert and Willis, 1957; and Zühlsdoff and Spieß, 2004). As increases in pore-fluid pressure cause fractures to form, similarly decreases in the pore-fluid pressures will result in their collapse. The formation of a fracture releases pore-pressure and as a result the fracture is assumed to close when pressures drop beneath the least principal stress (Luo and Vasseur, 2002). This process of propagating and collapsing fractures can repeat if the source of the over pressure is preserved. Vertical fractures can play an important role in an area's fluid migration system by increasing the porosity of a layer or providing direct pathways along which gas can travel (figure 5). Numerical models suggest micro-cracks connect to form networks of elongated fractures (Luo and Vasseur, 2002).

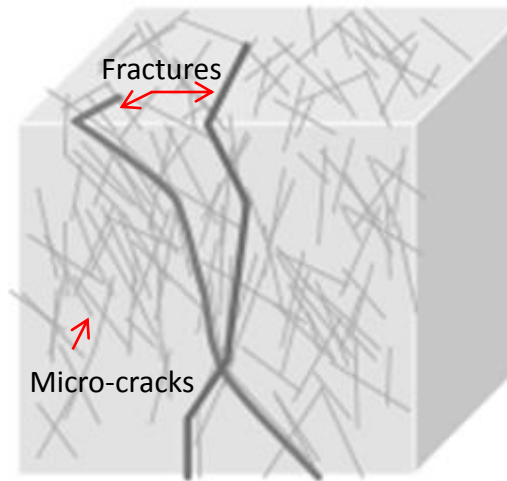


Figure 5: Model of micro-cracks within a medium connecting to form a fracture network (Modified with permission from Luo and Vasseur, 2002).

Natural fractures are also an important mechanism for methane migration within gas hydrate dominant environments, such as south Hydrate Ridge. Hornbach et al.

(2004) completed a study of critically pressurized gas reservoirs beneath multiple gas hydrate provinces and determined that most of the hydrate provinces have sufficient gas pressures to result in shear failure along favorably oriented faults. Flemings et al. (2003) determined that high lithostatic gas pressures at Blake Ridge, offshore SC, produce fractures by hydrofracturing, along which methane is actively migrating through the hydrate layers. They argued that the methane beneath Blake Ridge may be rapidly transported to the seafloor along these fractures, instead of being trapped within the GHSZ and forming hydrate.

This study determines the roles of over-pressured gas accumulations and natural fractures in migrating methane within the GHSZ. Specifically, this research presents evidence that accumulations of gas may result in the propagation of natural fractures through the GHSZ, which provide direct migration pathways to feed active seafloor vents at south Hydrate Ridge.

SOUTH HYDRATE RIDGE GEOLOGICAL SETTING

The focus area for this research on fluid migration, methane venting, and natural hydraulic fracturing within a gas hydrate environment is the southern knoll of Hydrate Ridge. Hydrate Ridge is a peanut shaped bathymetric high located on the Pacific continental shelf, within the Cascadia subduction zone's accretionary margin and roughly 60nm (80km) west of Newport, Oregon (figure 6). Both landward- and seaward-verging thrust-bounded anticlines characterize the Cascadia margin, with the transition zone between the two occurring offshore central Oregon (MacKay et al., 1992). South Hydrate Ridge is one of the N-S trending thrust-bounded ridges, located in the predominately seaward-vergence zone (figure 7). The tectonic and structural histories of

the ridge play an important role in the distribution of gas hydrates and methane migration, due to the varying age and permeability of the sediments within the GHSZ. Chevallier et al. (2006) determined through seismic sequence and structural analysis that initial accretion of sediment on the ridge occurred between 1.6 and 1.2 Ma. At ~1.2 Ma, activation along a landward thrust fault placed deep-sea fan sediments atop the previously accreted stratigraphy. The uplift of the southern ridge occurred around 0.3-0.2Ma along the reactivation of a seaward-verging fault (figure 8) (Chevallier et al., 2006). The accreted stratigraphy resulted in varying porosity, permeability, and grain size distributions within the GHSZ. The gas hydrate then developed preferentially within the porous, coarse-grained deep-sea fan complexes which were thrust up into the shallow GHSZ (Chevallier et al., 2006).

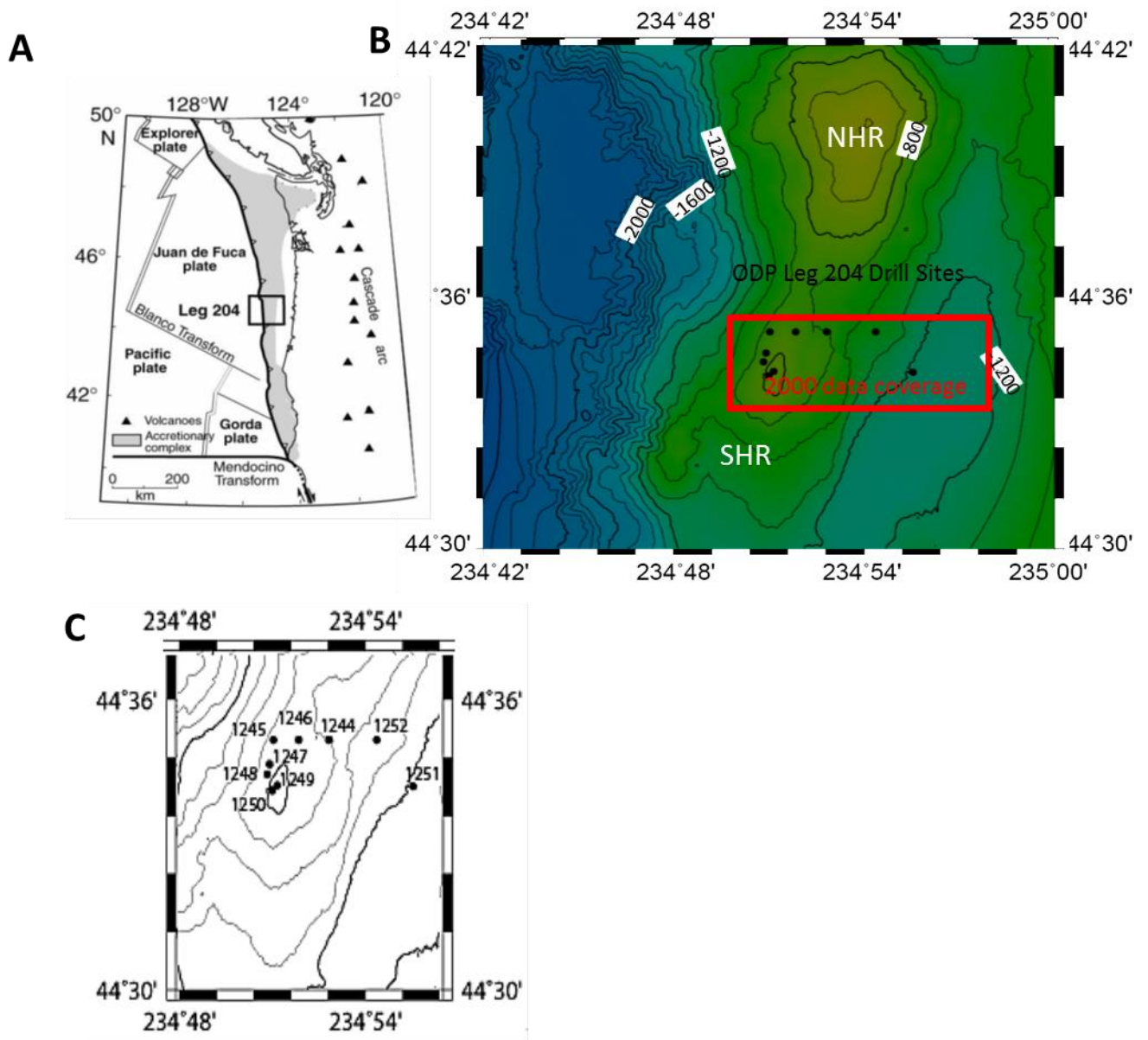


Figure 6: (A) Hydrate Ridge, located on the Cascadia accretionary margin (reprinted with permission from Torres et al., 2004) (B) drill sites from ODP Leg 204 as black circles and the approximate 3D seismic survey area shot in 2000 in red. (C) Zoomed in map of the ODP Leg 204 drill sites.

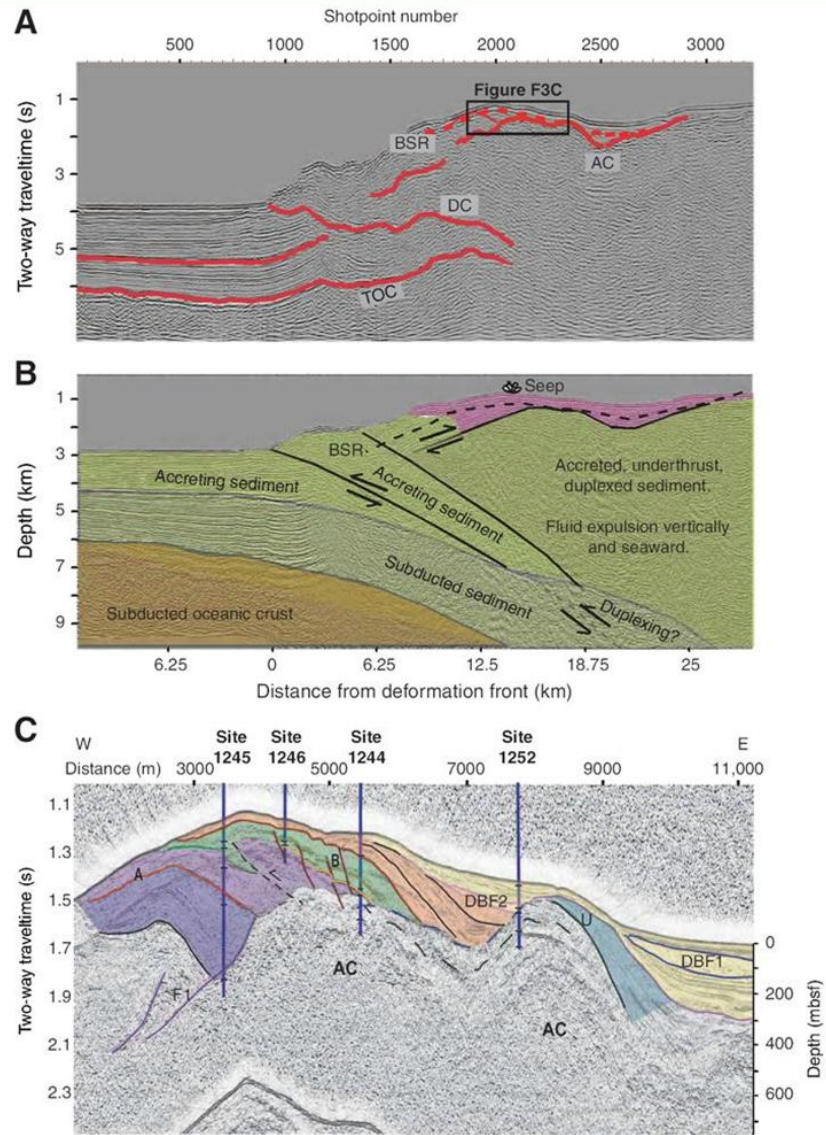


Figure 7: Previous seismic reflection profiles across south Hydrate Ridge (reprinted with permission from Tréhu et al., 2006). A) Regional profile OR89_line2 from ODP Leg 146 (originally from MacKay et al., 1992) showing the offshore Oregon accretionary complex. B) Interpreted seismic section from A converted into depth. C) Seismic slice from 3D survey acquired in 2000 that coincides with box in A (Tréhu et al., 2006).

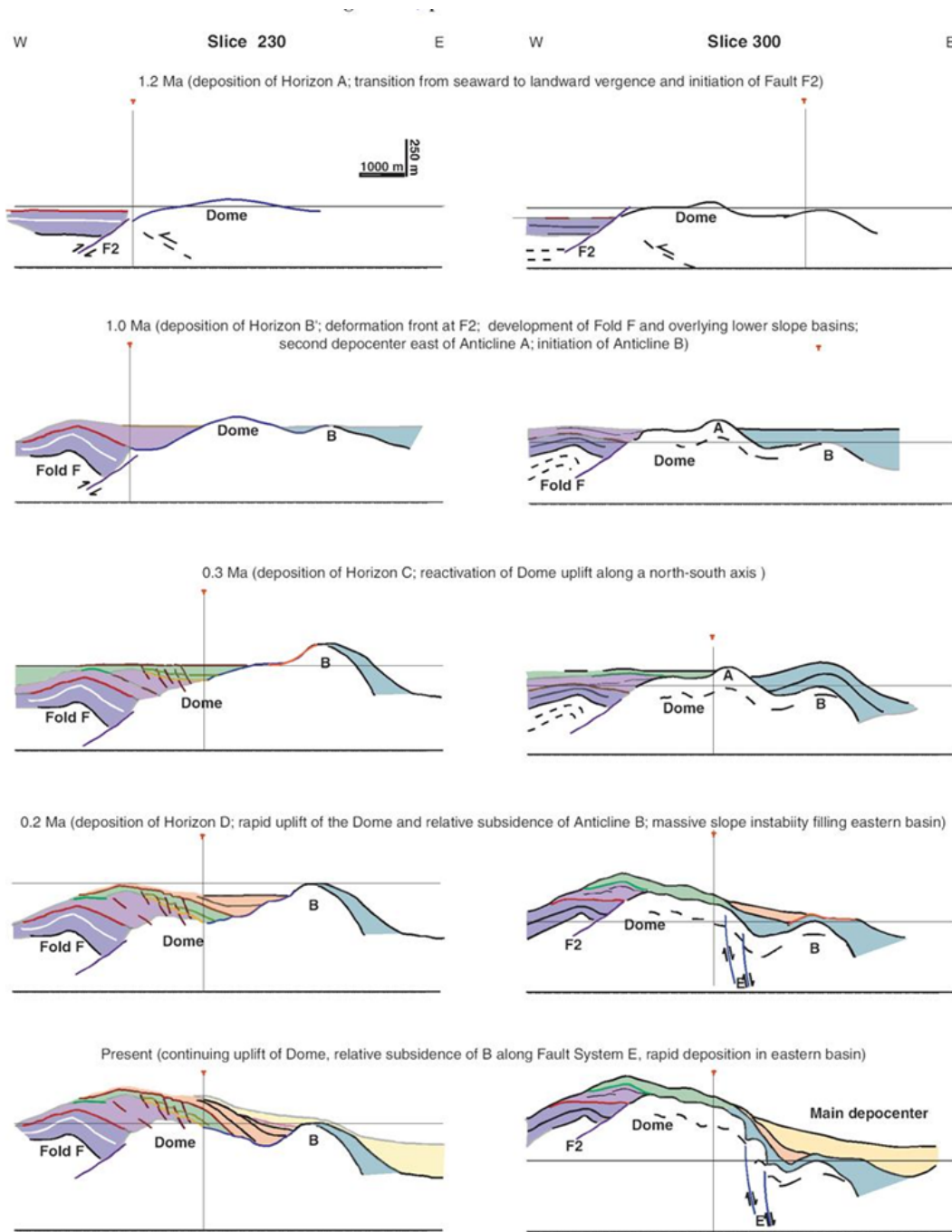


Figure 8: Tectonic evolution of south Hydrate Ridge based on the 2000 data, which is responsible for uplifting the deep-sea fan complexes (reprinted with permission from Chevallier et al., 2006).

The Ocean Drilling Program (ODP) completed Leg 204, including nine wells on and within the vicinity of south Hydrate Ridge (figure 6), as the first gas hydrate research driven ODP initiative to understand hydrate processes on an accretionary complex. The data collected from ODP Leg 204 at south Hydrate Ridge led to numerous research opportunities in the unique characteristics of gas hydrates and their geological setting. At south Hydrate Ridge, both gas hydrates and free gas seeps are observed at the seafloor (figure 9). Log data from leg 204 showed that the sediments at Hydrate Ridge are both highly porous and water saturated; under these conditions it is expected that all free gas will form hydrate (Tréhu et al., 2004b). Tréhu et al. (2004b) calculated gas saturation estimates using the density log data recovered on leg 204. They estimated intergranular density to be sufficiently low that pore space requires 68% free gas saturation in the pore space to account for the low intergranular density. They also noted that because methane needs such a large quantity of water to form hydrate (5.75 moles of water per mole of methane), once gas saturations exceed 68%, there is a sufficient quantity of free gas in pore space to consume all of the available water and convert it to hydrate. If we assume this is a closed system and there is little or no source of water migrating into these very low permeability sediments, free gas will coexist with the hydrate due to insufficient available water to convert any remaining free gas into hydrate. Furthermore, hydrate formation excludes salts, which also inhibit hydrate formation. The presence of these salts yields not only less hydrate, but also increases the stability of free gas within the hydrate stability zone. The high gas saturation and high salinity detected at Hydrate Ridge implies free gas and frozen methane hydrate very likely coexist (Tréhu et al., 2004b; Milkov et al., 2004; Liu and Flemings, 2006). Models of the hydrate formation showed that the current conditions at Hydrate Ridge must involve vertical migration of

free gas in order to produce the young massive hydrates at the surface (Torres et al., 2004). The models estimated that the hydrates are at most, 1500 years old, and are forming at rates of $10^2 \text{ mol m}^{-2} \text{ year}^{-1}$ (Torres et al., 2004).

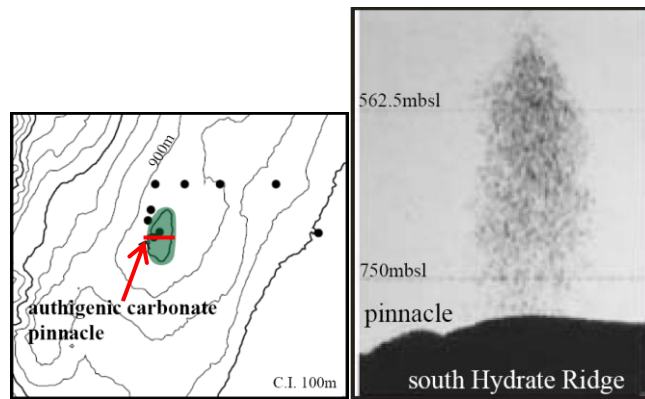


Figure 9: (left) The summit of south Hydrate Ridge is characterized by an authigenic carbonate pinnacle and seafloor gas seeps, approximate seep area shown in green. (right) An acoustic image (modified from Heeschen et al., 2003) of free gas venting from the summit of south Hydrate Ridge, with an approximate line location shown in red.

Hydrate Ridge's two topographic highs (S. and N. Hydrate Ridge) are characterized by gas vents and seeps that were observed with previous ODP drilling, fluid flow monitoring, seafloor bathymetric surveys and seismic surveys including a 3D seismic survey in 2000 (Chevallier et al., 2004; Tréhu et al., 2004a; and Tréhu et al., 2006). On the eastern flank of the ridge's southern summit, there is an authigenic carbonate pinnacle observed by seismic and bathymetric imaging (Tréhu et al., 2006). Authigenic carbonate is related to methane venting and may indicate former migration pathways that are no longer active (Teichert and Bohrmann, 2006).

The 2000 3D seismic volume imaged an anomalously-bright feature, "Horizon A", that is continuous from the accretionary complex to the summit of south Hydrate

Ridge and may contribute to stratigraphic migration of free gas (figure 10) (Tréhu et al., 2004a). Drilling sites 1245, 1247, 1248 and 1250 found that Horizon A is a 2-4 m thick turbidite layer with abundant volcanic ash and is gas saturated (Tréhu et al., 2004a). Data from LWD logs (figure 11) showed Horizon A as having anomalously coarse grain size (20% clay compared to 50-60% clay of overlying sediment) and low bulk density (1.4g/cm^3 compared to 2.2 g/cm^3). The chemistry of the gas sampled at sites 1245 and 1247 showed anomalously low C1/C2 and high $\delta^{13}\text{C}$ at Horizon A, indicative of migrated deeply sourced thermogenic gas in Horizon A and biogenic gas in the GHSZ (figure 11) (Tréhu et al., 2006). This horizon can be mapped continuously for over 3km^2 . The negative seismic reflection amplitude is brightest below the summit and weakens below 1060mbsl as the horizon dips north (figure 12). The logging results, along with the bright negative polarity, suggest that free gas is present in the pore space above 1060mbsl (Tréhu et al., 2004b).

The scientific party of Leg 204 identified various ranges of hydrate concentrations on and beneath the seafloor of south Hydrate Ridge from core samples, seismic reflection data, and LWD results. Gas hydrates were recovered at sites 1244-1251 as lenses and nodules within coarse-grained stratigraphic units, ranging from millimeter deposits to several meter thick clusters (Tréhu et al., 2006). A statistical correlation between grain size and hydrate presence indicated that the hydrates preferentially form within the silty and sandy turbidite deposits rather than the surrounding hemipelagic deposits (Tréhu et al., 2006). Hydrates within the turbidite deposits are nodular with sub-millimeter to centimeter thicknesses, however they occur in heterogeneous clusters, massing to several meters thick (Tréhu et al., 2006).

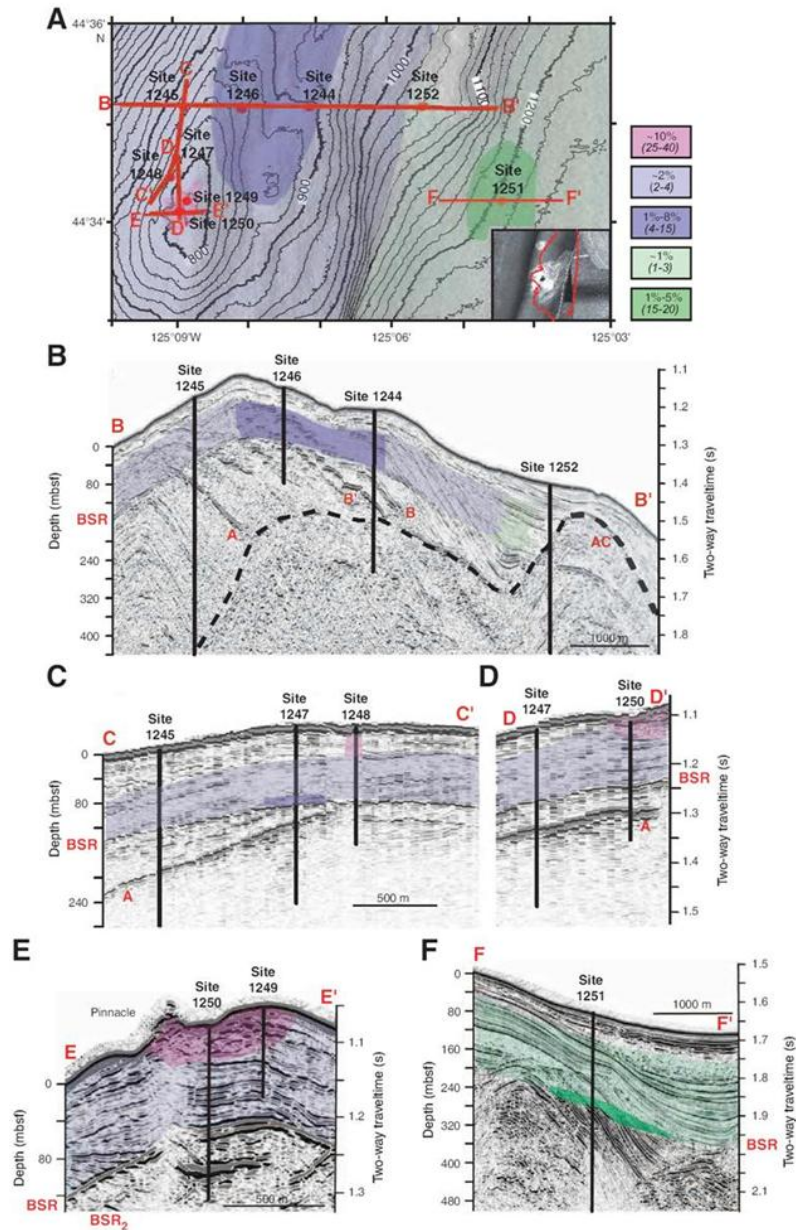


Figure 10: Hydrate concentrations (colored overlays) at south Hydrate Ridge from the 2000 3D reflection volume. The map represents hydrate concentration averaged from the seafloor to the BSR. The anomalously bright Horizon A is also apparent on B, C, D, and E cross sections (reprinted with permission from Tréhu et al., 2006).

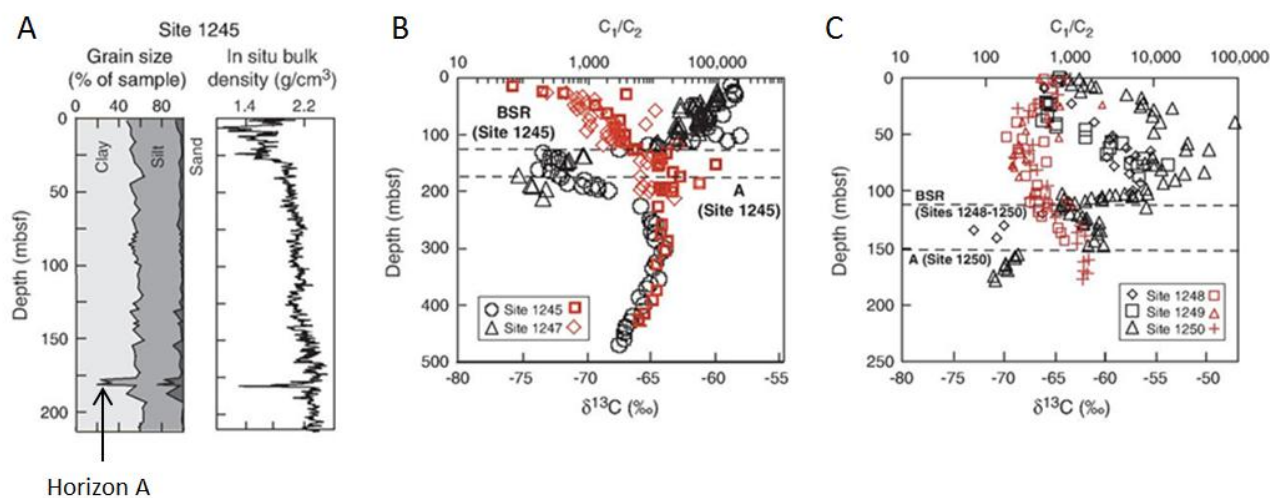


Figure 11: A) LWD in situ bulk density and grain size distribution at site 1245, showing anomalous Horizon A at ~175mbsf (reprinted with permission from Tréhu et al., 2004b). B) C_1/C_2 ratio and isotopic composition of methane at sites 1245 and 1247, showing low C_1/C_2 and high isotopic composition at Horizon A, indicating migrated gas. Gas chemistry within the GHSZ is indicative of biogenic gas (reprinted with permission from Tréhu et al., 2006). C) Chemistry of methane at the summit, indicating migrated gas in Horizon A and the upper 20-30mbsf. (reprinted with permission from Tréhu et al., 2006).

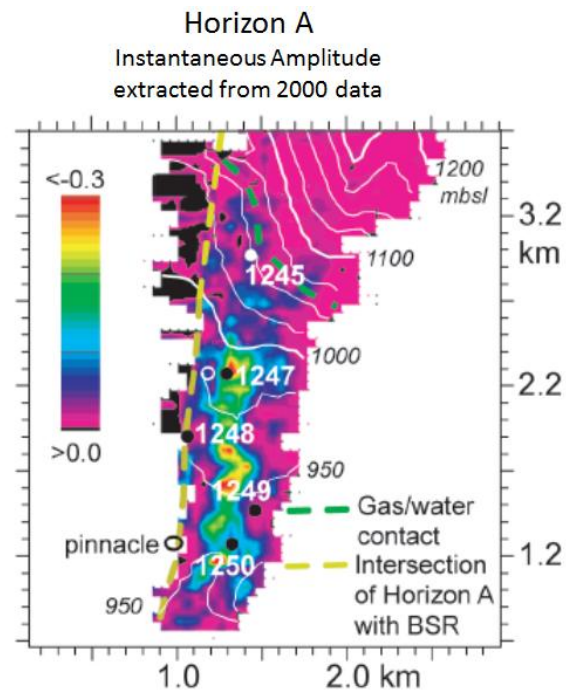


Figure 12: Amplitudes of Horizon A extracted from the 2000 data volume, showing the gas-water contact in dashed green and the BSR and Horizon A intersection in dashed yellow (reprinted with permission from Tréhu et al., 2004b).

South Hydrate Ridge has favorable conditions for vertical fracturing in the shallow subsurface. Tréhu et al. (2004b) interpreted the normal faulting observed at south Hydrate Ridge's summit to indicate a local tensional environment, although the ridge is located along a major convergent margin. These tensional forces could create vertical fractures and allow free gas pass through permeable layers if connected by faults (Tréhu et al., 2004b). High pore-fluid pressures sampled from the summit of south Hydrate Ridge may also be a factor in creating vertical fractures that allow gas migration to the surface (figure 13) (Cochrane et al., 1994; and Tréhu et al., 2006). Vertical gas effective stress at the summit is low, ranging from 0.2MPa to -0.2MPa, as calculated from the logs collected during ODP Leg 204 (figure 13) (Tréhu et al., 2006). When the vertical gas effective stress is zero, it is interpreted that the pore pressure has reached or exceeded the least principal stress, resulting in hydraulic fracturing.

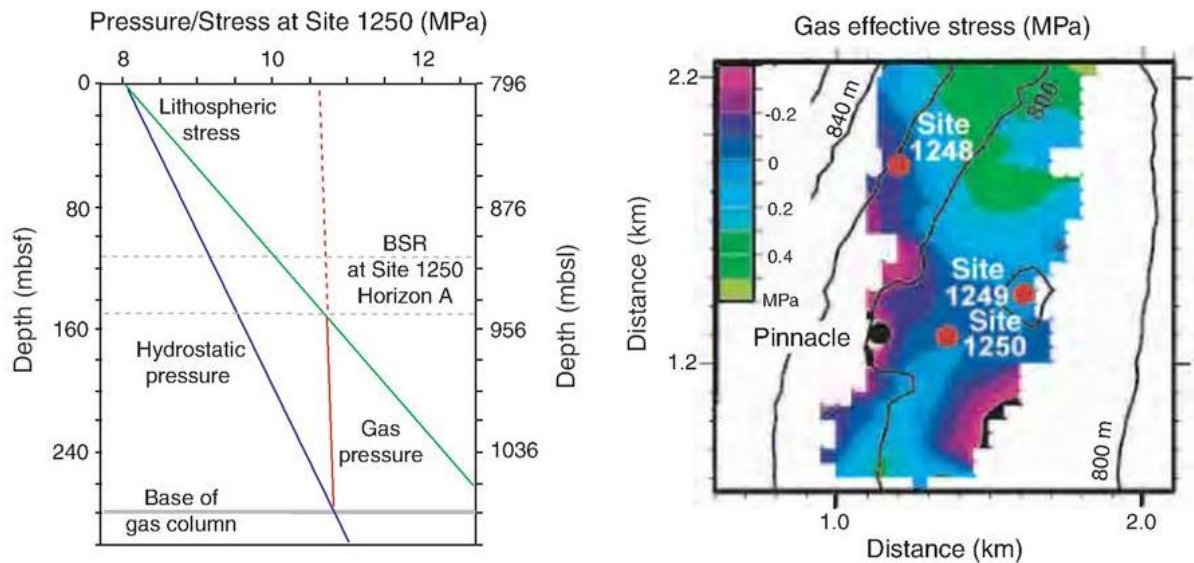


Figure 13: Gas pressure at site 1250 and gas effective stress mapped along south Hydrate Ridge's summit (reprinted with permission from Tréhu et al., 2004b).

OBJECTIVES

The primary objective of this thesis is to identify and characterize the complex methane migration system beneath south Hydrate Ridge. South Hydrate Ridge is an excellent candidate for an analysis on fluid migration within a hydrate environment because of the high gas saturations, large quantities of gas hydrate, and active seafloor seeping. The members of the RV Thompson TTN220 Scientific Party collected a new high resolution seismic reflection data volume, described in detail in Chapter 2, to image the subsurface and aid in characterizing the plumbing system of south Hydrate Ridge. Chapter 3 investigates the origin of the methane sampled from south Hydrate Ridge and supplements the previous analysis of methane present in Horizon A with interpretations from the new data volume. Chapter 4 utilizes new interpretations from the 3D volume to identify potential migration pathways within the gas hydrate stability zone, which are supplying methane to the subsurface gas hydrate accumulations and the seafloor vent sites. A synthesis of the methane generation, migration and hydrate formation is discussed in Chapter 5. Finally, the results of this work are summarized in Chapter 6.

Chapter 2: 3D Seismic Reflection Data

SEISMIC ACQUISITION

The data I used in this thesis were acquired by the members of the RV Thompson TTN220 Scientific Party. They acquired a high resolution three dimensional seismic reflection data set during the summer of 2008 over the southern ridge of Hydrate Ridge, offshore Oregon. The survey area is approximately 60 nautical miles (80km) west of Newport, Oregon on the southern knoll of Hydrate Ridge (Figure 14). The data volume covers a 3x6km area that extends N-S from the saddle separating the north and south ridges to the summit of the southern ridge. This area runs perpendicular to the previous 3D seismic reflection volume collected in 2000 over south Hydrate Ridge and covers 6 of the 9 ODP Leg 204 drill sites, sites 1245-1250.

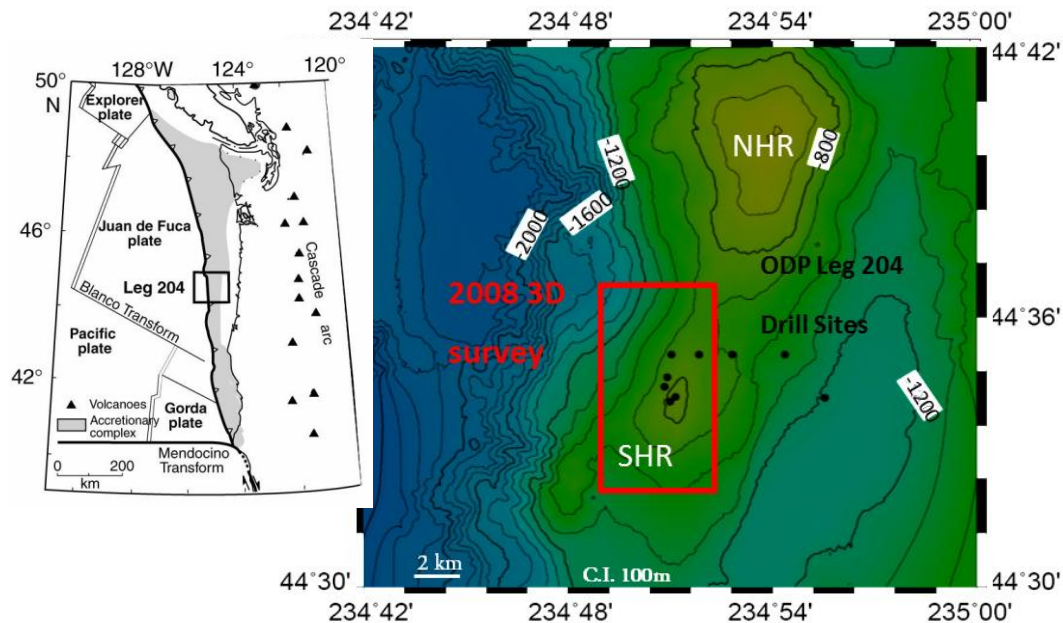


Figure 14: Survey area for the south Hydrate Ridge 2008 3D seismic reflection volume (regional inset reprinted with permission from Torres et al., 2004).

The survey was acquired using the P-Cable system to provide the highest resolution image of the uppermost 1000m beneath the seafloor where a complex environment of free gas venting and methane hydrate formation is present. They acquired these data to better understand how free methane migrates through the subsurface, particularly the gas hydrate stability zone, to the active seafloor vents and to determine the relationship between the migrating methane and the hydrates.

P-Cable System

The P-Cable is a marine data acquisition system that produces a low fold, high seismic resolution data volume using a series of single-channel streamers. It was created by the Volcanic Basin Petroleum Research (VBPR) in collaboration with the National Oceanography Centre of South Hampton (NOCS), the University of Tromsø (UiTø) and Fugro Survey AS, Oslo. This survey was the first to use the P-Cable prototype system, provided by NOCS.

In the NOCS P-Cable configuration (figure 15), two reinforced power cables of 80m length extend from the boat to a pair of paravanes. These paravanes are connected by a cable perpendicular to the boat, on which several, up to 12, single-channel streamers are attached. The paravanes and a buoy in the center of the cable help maintain the streamers at 12.5m spacing and 2-5m depth. Each paravane has a GPS receiver that transmits back to the boat.

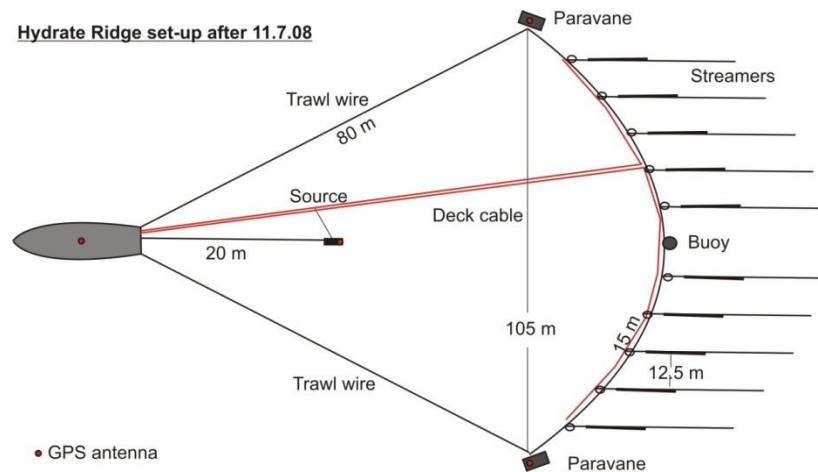


Figure 15: P-Cable set up, utilizing 10 single-channel streamers, which was used to acquire the 2008 3D seismic volume.

Acquisition Parameters

The 3D high resolution survey at south Hydrate Ridge ("HR3D08") was collected using the R/V Thompson from June 30th to July 15th of 2008. The survey volume consists of 56 N-S lines, 5km in length plus turns with 50m line spacing, to cover a total 3x6 km area. Four E-W lines were also acquired during the duration of the seismic cruise. The P-Cable system, described above, used 10 Teledyne Geophysical Instruments analogue streamers with a single hydrophone per streamer. The streamers were separated by 12.5m, totaling to 62.5m coverage over the ground. The Lamont-High-Res system GI array, which consists of two 75/75 cu in air guns towed at 2m depths, served as the seismic source for the survey. The guns, arrayed so that one was towed directly behind the other, were fired in 6s intervals and had a total volume of 300 in². The GI airguns utilized 1800psi air pressure. The survey used Seadiff's Kongssber Seatex RGPS tracking system for the positioning equipment and the Gemetrics Geode 24 system for the seismic recording and on board data digitization.

The final 3D seismic survey volume consists of 220 inlines and 700 crosslines with a 3 second record length. The data were recorded at a 0.5ms interval, totaling to 6000 samples. The dominant frequency of the reflection data in the volume is 70Hz. The Nyquist frequency is 1000Hz (figure 16). The vertical resolution of the data is approximately 2-2.5m. This high resolution allows for a detailed interpretation of the complex shallow structures of the subsurface gas migration system beneath Hydrate Ridge which has previously been unknown. A high vertical resolution survey was necessary because the gas is likely migrating through a 20ms (~300m) thick section between the BSR and the seafloor.

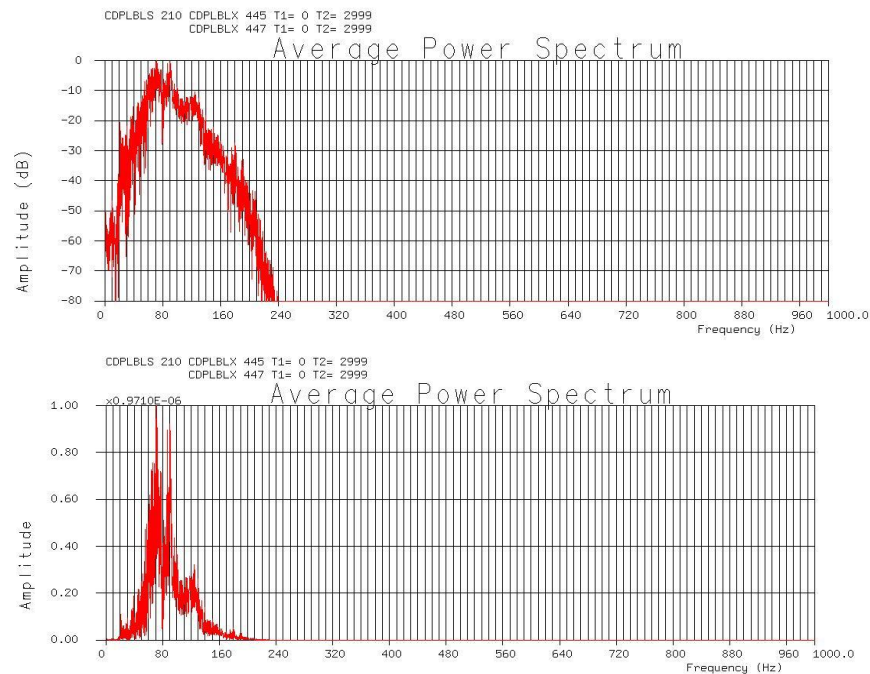


Figure 16: HR3D08 data frequency in amplitudes scaled to decibels (top) and linear scaling (bottom).

SEISMIC DATA PROCESSING

The processing sequence for the HR3D08 seismic reflection data volume is detailed in the section below. Only minimal processing and noise filtering were needed with the new P-Cable prototype acquisition parameters. I used Paradigm Geophysical's FOCUS software as the main tool for the seismic data processing. The main objective of the processing was to enhance the signal to noise ratio while maintaining the low frequency reflections, which provided a higher image resolution when compared to previously collected data volumes.

The first step towards processing the data volume involved calculating the midpoint between the source and receiver for each trace, from which I determined the individual reflection point positions. I then assigned inline and crossline values to each trace based on the position of the reflection points and sorted all of the traces in the inline direction. The traces were binned into 12.5m by 12.5m size bins and stacked. Figure 17 displays the fold, or data coverage, for the binned survey. Data fold ranged between 4-8 traces per bin throughout most of the survey area, but some higher fold exists in the critical areas around the south summit. Data coverage was greatest in the center of the volume to provide the best resolution of the ridge's summit.

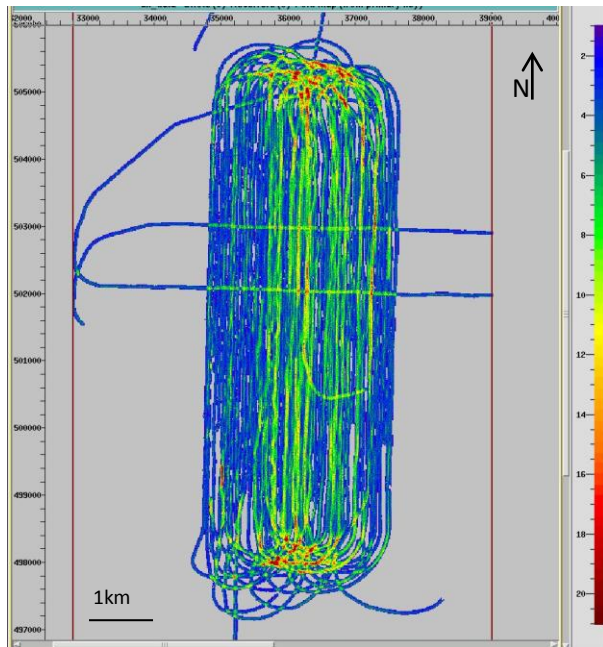


Figure 17: Fold map displaying the survey's data coverage. On average the bins contained between 4 (blue) and 8 fold (green), with a maximum of 18 (red).

An applied bandpass filter eliminated frequencies outside the designated signal range 25Hz - 180Hz (figure 18). This reduced noise generated from the water column, electrical or instrumental noise, and high frequency noise. A despiking tool in FOCUS reduced spike noise (figure 19).

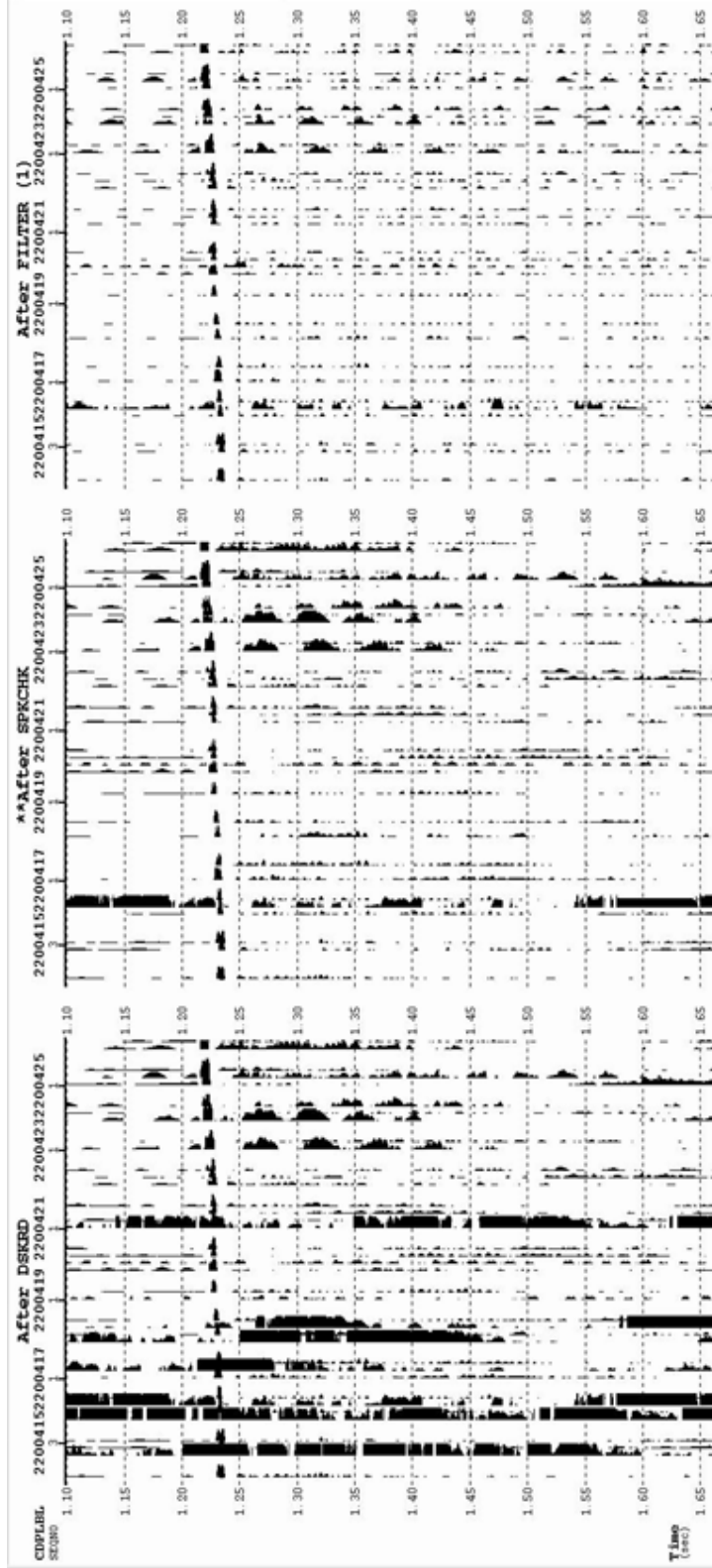


Figure 18: Noise reduction comparisons on (a) a single shot gather using (b) a de-spiking tool and (c) a trapezoidal bandpass filter (1,25,180,250).

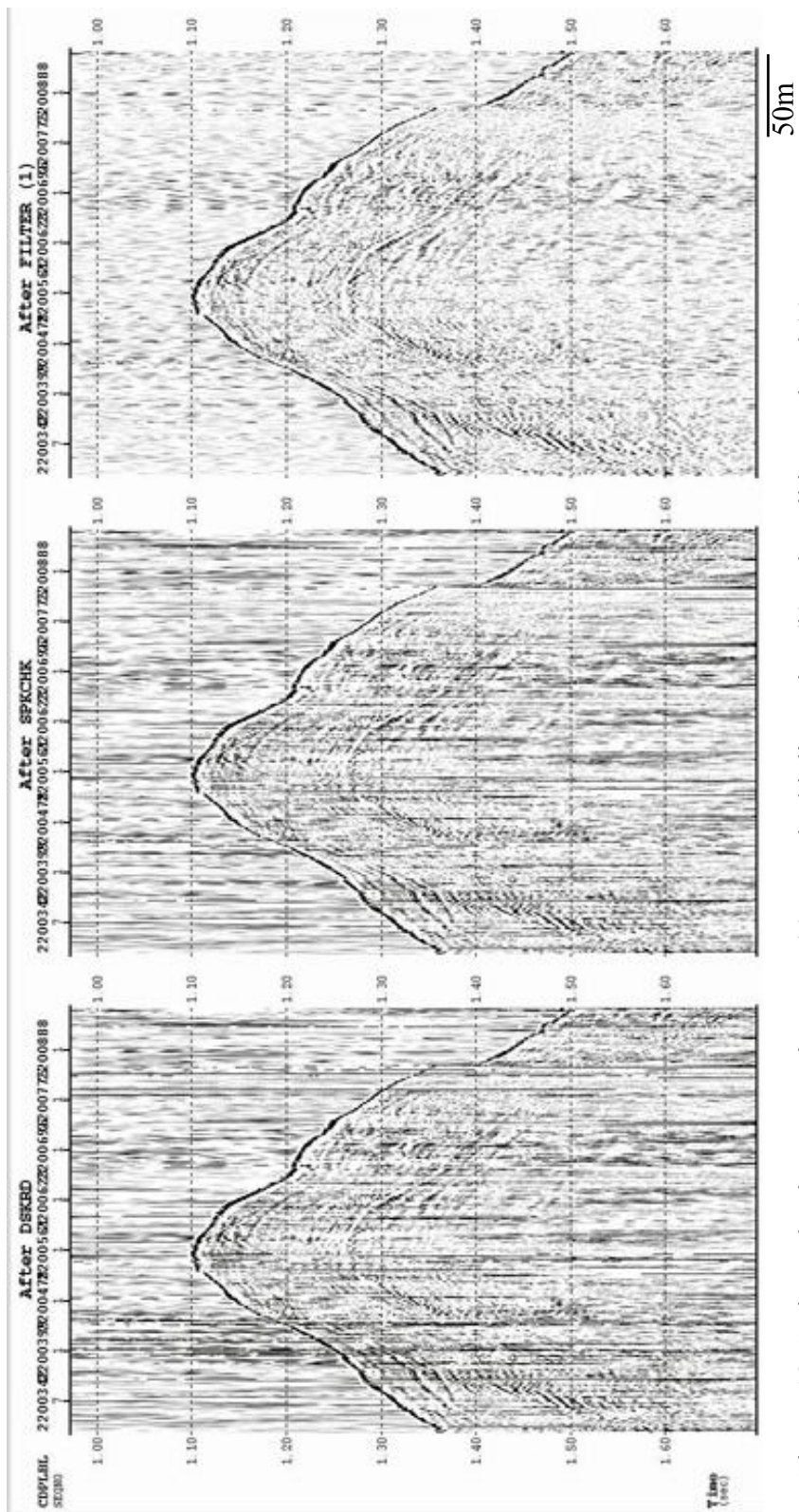


Figure 19: Noise reduction comparisons on (a) a stacked inline using (b) a de-spiking tool and (c) a trapezoidal bandpass filter (1,25,180,250).

The final stack was reorganized by crossline and the traces were interpolated in the crossline direction to fill any gaps in the data coverage. Finally, the stacked 3D volume was migrated using the Kirchhoff post-stack 3D migration with a velocity model of 1500m/s (figure 20). The final stacked and migrated data volume was used for interpreting the structural features beneath south Hydrate Ridge. The migration improved the resolution of the detailed shallow subsurface beneath the ridge and improved the image of deeper reflections that were not seen on the original stack, as seen on figure 19. The red arrows on figure 19 designate reflections at roughly 1.45s that are enhanced in the migrated volume and are not visible in the original stack.

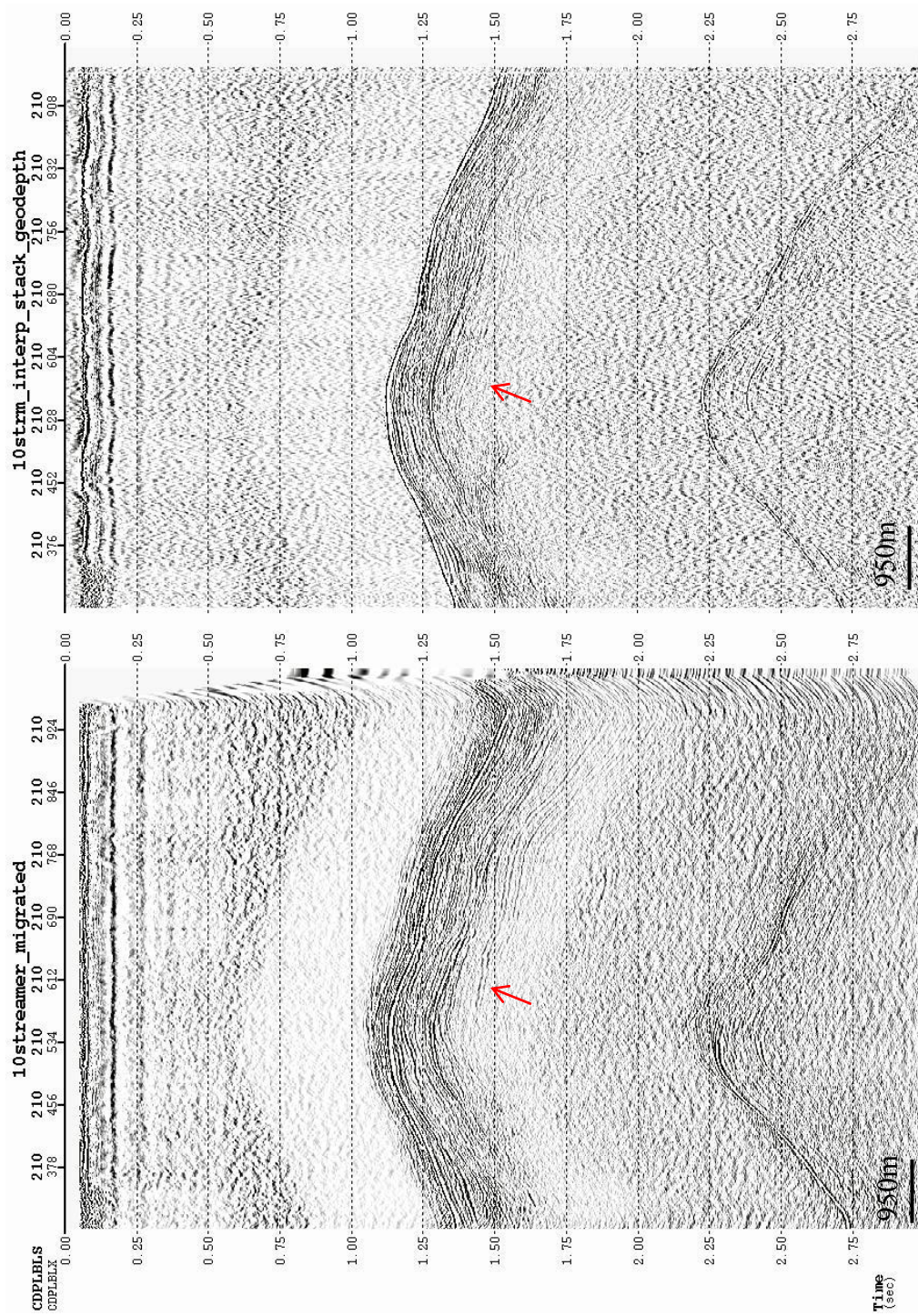


Figure 20: (Left) Migrated stack of crossline 210, using a Kirchhoff post-stack 3D migration with a velocity model of 1500m/s (Right) Un-migrated stack of crossline 210. Red arrows designate examples of reflections enhanced through migration.

INTERPRETATION STRATEGIES & OBSERVATIONS

The following section describes the interpretation methods and strategies used to interpret the HR3D08 high resolution data volume as well as key observations made. I used Paradigm Geophysical's GeoDepth and VoxelGeo 3-dimensional seismic reflection interpretation software packages to interpret the data volume. I primarily utilized GeoDepth's imaging, amplitude extraction, and horizon and fault picking tools for interpreting the geological structures beneath south Hydrate Ridge. The 3-dimensional imaging and opacity features of VoxelGeo presentation software provided additional interpretational resources to confirm each structure.

Several distinct observations can be made from the HR3D08 data volume. First and most prominent, is a continuous and anomalously bright amplitude reflection that follows the seafloor, roughly 160msbsf on average (figure 21). This bottom-simulating reflection, or BSR, has a reversed polarity to that of the seafloor reflection. The BSR is continuous beneath the entire southern ridge (figure 22 and 23). This is consistent with observations from the previous reflection seismic survey in 2000 (Tréhu et al., 2004b; and Chevallier et al., 2006). A second observation is that the reflection signal penetration is good until roughly 1.4s, after which reflections become more difficult to fully resolve and interpretations at these depths are less confident (figure 21). The seismic signal penetrates deeper in the earlier 2000 seismic reflection data volume and the resolution of deeper reflections is better compared to the new survey. The resolution of the shallow subsurface on the new 2008 seismic survey is higher and therefore features can be mapped in greater detail than previously accomplished on the 2000 data. With a higher resolution of the shallow features, I observed that the shallow subsurface (<200msbsf) is characterized by multiple, non-continuous reflections that vary laterally in amplitude

(figure 24). A separate, anomalously bright amplitude reflection was imaged beneath the BSR at roughly 200ms below the summit of the ridge and dipping north (figure 25). The spatial extent of this reflection, mapped as Horizon A, is shown in figure 26.

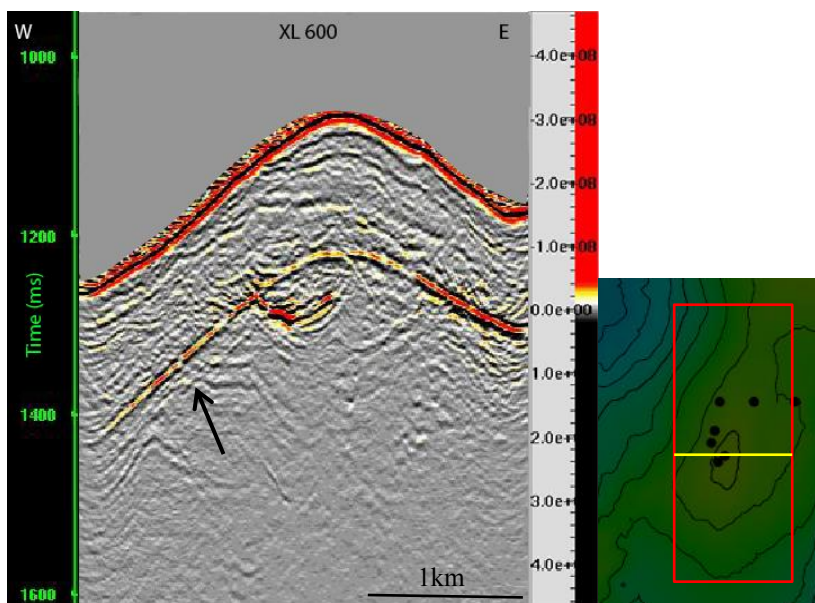


Figure 21: Crossline 600 showing a prominent, continuous bright amplitude reflection beneath the seafloor (shown by arrow) and loss of signal beneath ~1.4s.

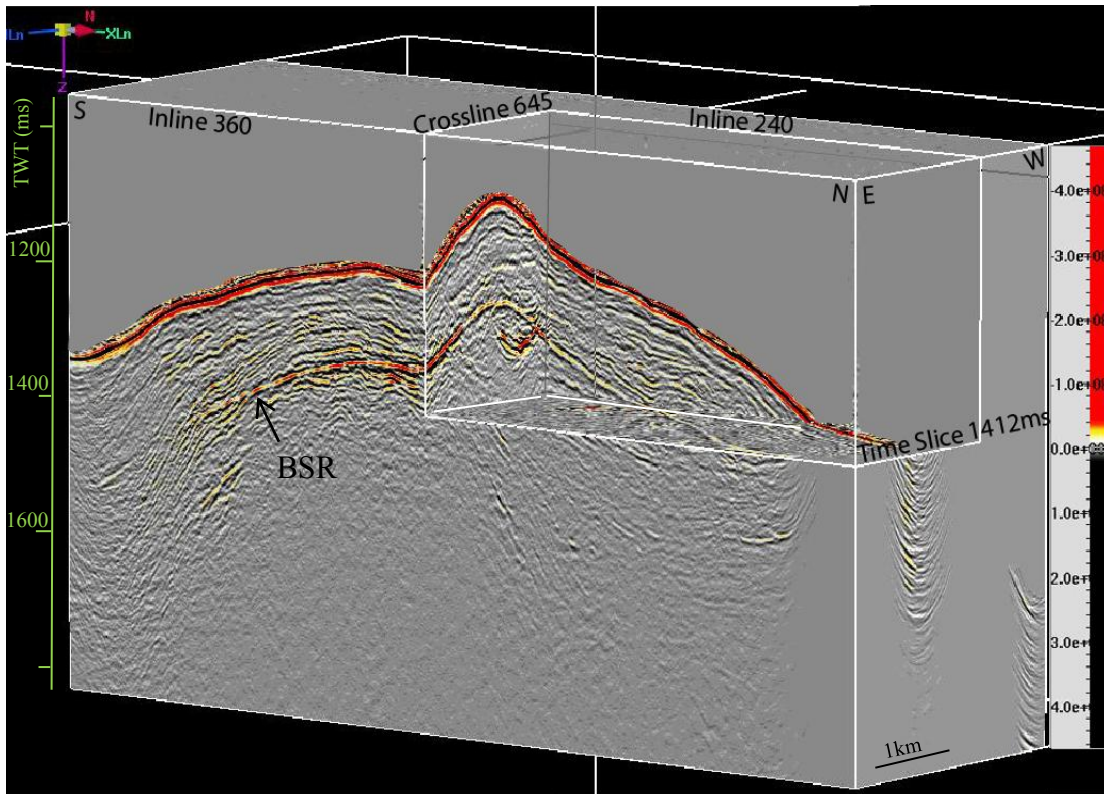


Figure 22: A cut-away 3D cube view showing a prominent, continuous bright amplitude reflection of the seafloor and the BSR beneath the seafloor.

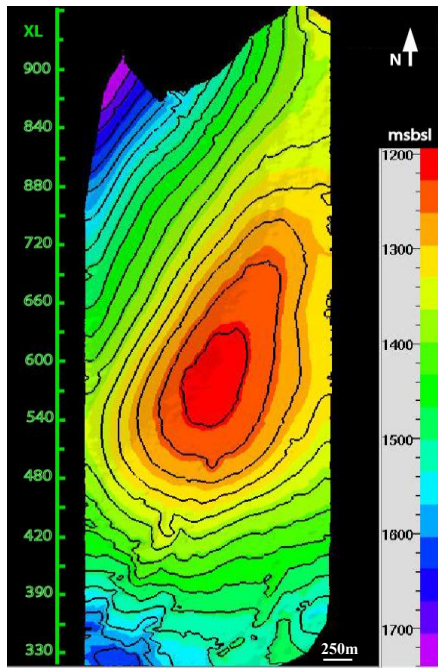


Figure 23: Depth map in msbsl of BSR (contour interval of 30ms).

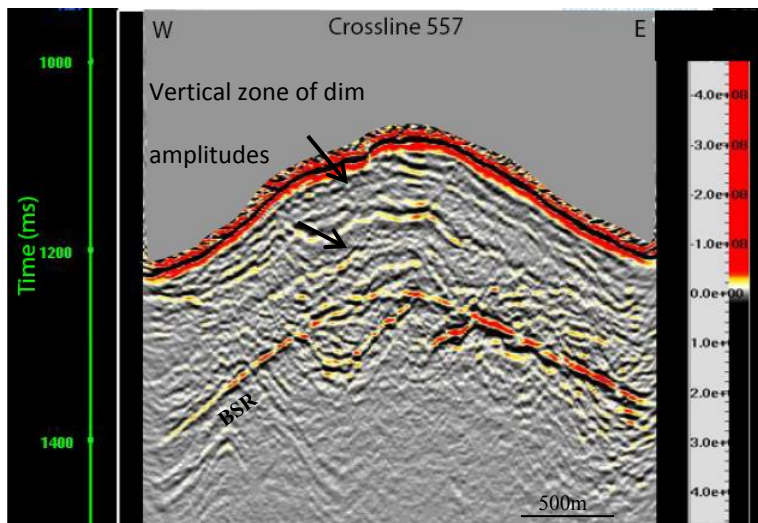


Figure 24: Crossline 557, depicting multiple, non-continuous reflections that vary laterally in amplitude and a blank-out zone of dim amplitudes.

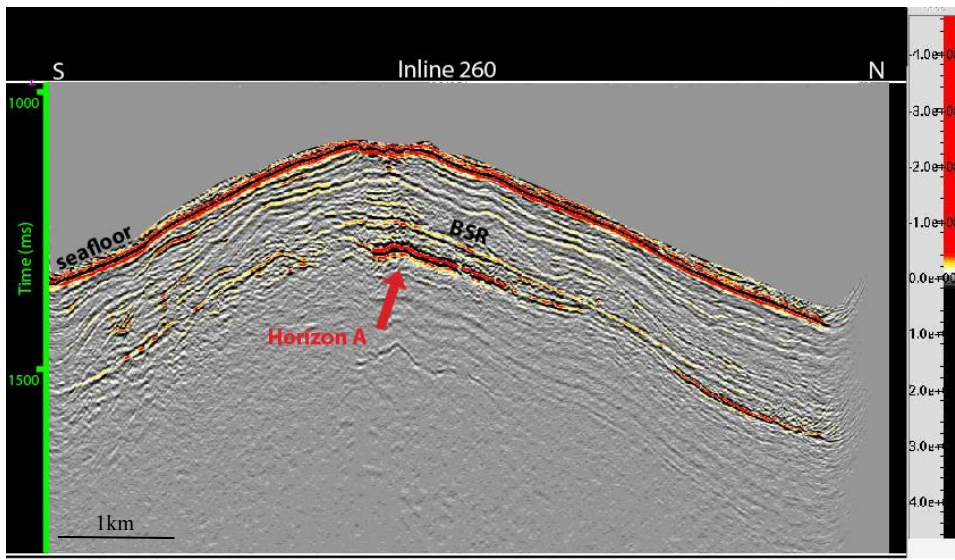


Figure 25: Inline 260 showing an anomalously bright amplitude north-dipping reflection imaged below the BSR called Horizon A.

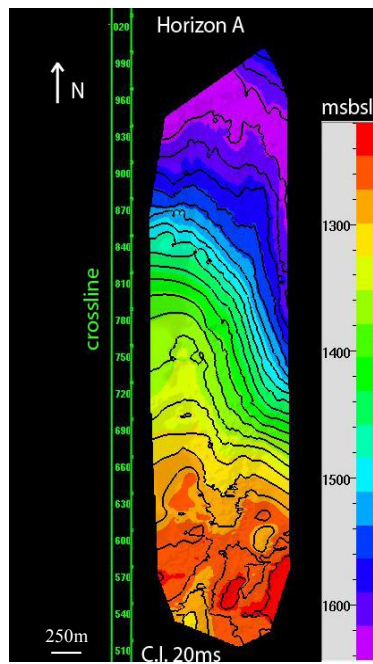


Figure 26: Depth map in msbsl of Horizon A (contour interval of 20ms).

In the HR3D08 seismic volume, the shallow subsurface (<50msbsf) contain numerous near-vertical discontinuities in horizontal reflections, including horizontal displacement along reflections, abrupt truncation of bright amplitudes, and vertical blank-out zones where the amplitudes are dim (figure 24). Other visible discontinuities include vertically offset reflections by a minimum of 3ms offset. These discontinuities are not limited to a single region of the survey, and are predominately N-S trending. Both sets of observed discontinuities are discussed in further detail in Chapter 4. This is the first time such features have been observed at south Hydrate Ridge because of the improved resolution of the subsurface in the new 3D survey.

FOCUS was used to extract the signal attribute, instantaneous amplitude, along the mapped surfaces of the seafloor, the BSR, and Horizon A. This attribute shows the lateral variations in reflection amplitudes along the mapped surfaces of the BSR and Horizon A (figure 27). The variations in amplitudes extracted along the seafloor are artifacts caused by the data coverage, where areas with a higher fold have brighter amplitudes. For this reason, the seafloor amplitudes were not useful for interpretational purposes. The amplitude extraction on the BSR shows isolated linear areas of higher amplitudes beneath the ridge summit that trend SW-NE (figure 27). The amplitudes along Horizon A are also brightest beneath the summit but are spatially continuous rather than having the linear trend observed on the BSR amplitudes. Horizon A's amplitudes dim as the reflector dips to the north; however there is a second area of bright amplitudes at the northern extent of the survey (figure 27). The northern zone of bright amplitudes on Horizon A had not been identified prior to this research.

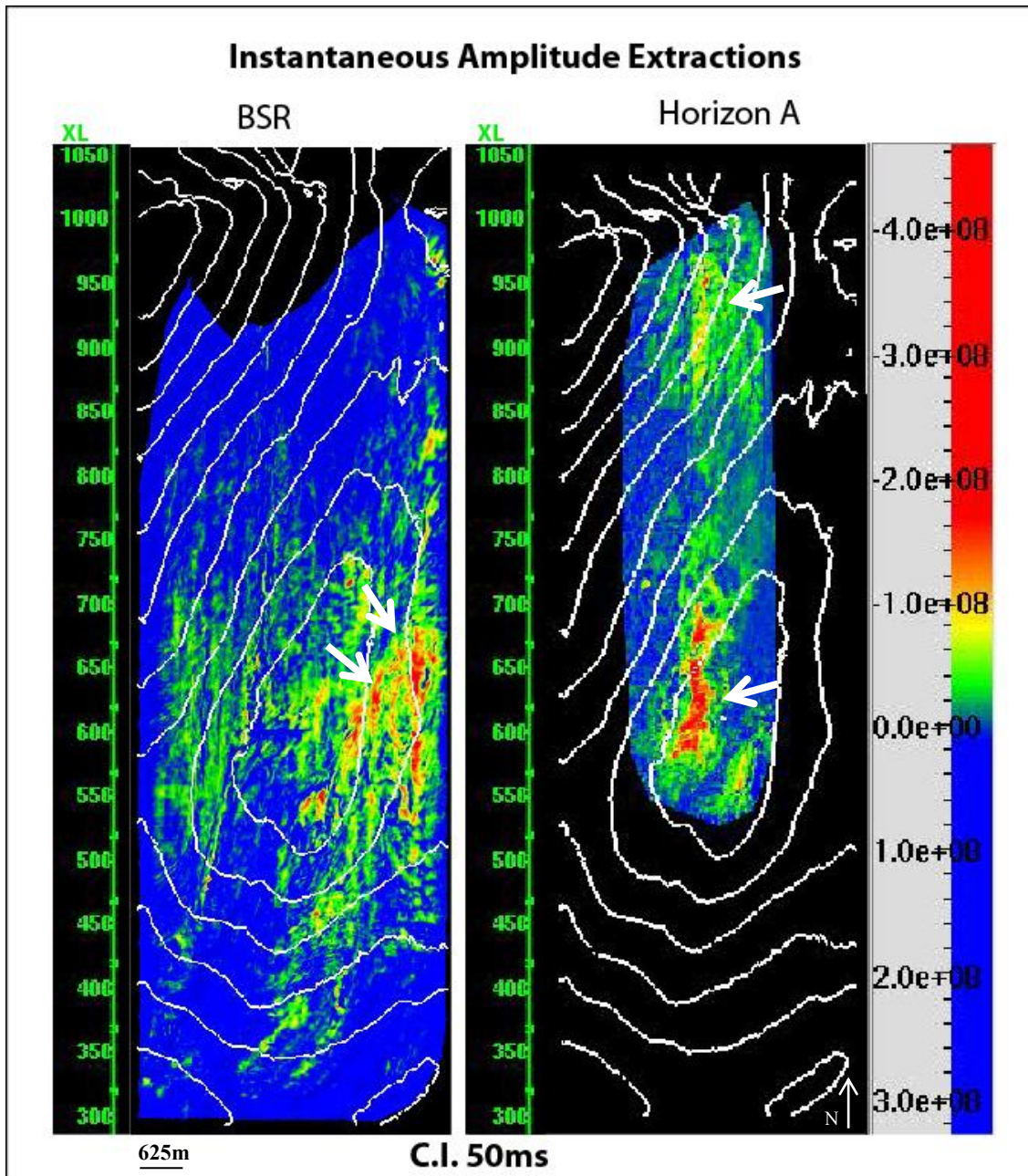


Figure 27: Instantaneous amplitudes of BSR (left) and Horizon A (right) with the seafloor contour overlay (50ms interval) in white. Note the incidences of high amplitudes (shown by white arrows) along the BSR on the eastern flank of the ridge and those on Horizon A, at the summit and on the northern flank.

The observed discontinuities in the seismic reflections and the variations in amplitude brightness of the BSR and Horizon A may relate to the fluid migration processes occurring at south Hydrate Ridge. In the following chapters, each of these observations is analyzed and interpreted in the context of active methane migration throughout the subsurface. Previous research at south Hydrate Ridge infers lateral migration of methane within porous sediment layers, such as the uplifted deep-sea turbidite deposits (Tréhu et al., 2006). Using the new 2008 3D seismic data, I interpreted the key horizons previously identified on the 2000 data volume and interpreted the new observations that were previously unresolvable on other seismic surveys. The following chapters describe my interpretations of the above observations, which yielded new insights on the lateral gas migration within Horizon A and the role of high pore-fluid pressures on natural fracturing beneath south Hydrate Ridge.

Chapter 3: Gas Supply System

Methane origin and transportation are important factors in the fluid migration system of south Hydrate Ridge. The origin of methane, whether it is biogenic or thermogenic, provides insight into the extent of migration occurring within the system. For instance, if the methane sampled at Hydrate Ridge is primarily biogenic in origin, then the fluids are generally generated from organisms in shallow depths and have not migrated from outside Hydrate Ridge's shallow gas hydrate environment (Hedberg, 1979). If the methane is identified as thermogenic in origin, then it was created at much greater depths than biogenic methane through compaction and heating of organic material. This form of methane must utilize migration networks or conduits to reach the depth of the GHSZ in Hydrate Ridge (Hedberg, 1979).

METHANE ORIGIN

During the ODP Leg 204 initiative, nine drilling sites were sampled using standard LWD tools, infrared core scans, and in situ pressure logging (Tréhu et al., 2006). High gas saturations were observed at well depths that corresponded to the seismic interpretation of Horizon A (figure 28) (Tréhu et al., 2004b). An analysis of the methane sampled from the sites revealed different chemical compositions of gas within the GHSZ and gas within Horizon A (Tréhu et al., 2006). These variations in C1/C2 and $\delta^{13}\text{C}$ indicated biogenic methane within the GHSZ and thermogenic methane within Horizon A (figure 11) (Tréhu et al., 2006). The source rock for the thermogenic methane is not observed in the ODP drill sites, the previous 2000 data (Chevallier et al., 2006), or our 2008 seismic survey, and is therefore presumed to be located deeper than 600mbsf. The thermogenic methane is assumed to have migrated to Horizon A from the source rock

along deep penetrating faults and permeable stratigraphic layers, and implies a gas migration system that connects the deeply sourced thermogenic methane to the shallow gas vent system at the south summit of Hydrate Ridge. The influx of gas to south Hydrate Ridge will affect possible fracture development and the activity of seafloor vents.

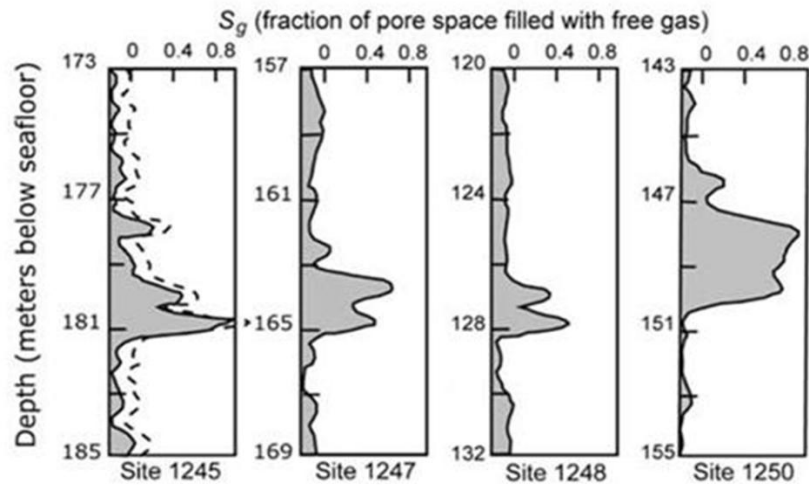


Figure 28: Gas saturation (S_g) for ODP sites 1245, 1247, 1248, and 1250 calculated by Tréhu et al. (2004b) using LWD bulk density logs and average porosity and density from moisture and density measurements. The depths of the observed high gas saturations correspond with the seismically imaged Horizon A (reprinted with permission from Tréhu et al., 2004b).

Evidence for thermogenic methane origin within Horizon A is consistent with the regional trends of the Cascadia margin. Thermal properties at the Cascadia subduction zone are anomalously high ($2.86 \mu\text{cal}/\text{cm}^2 \text{ sec}$ heat flow) when compared to the global average ($1.5 \mu\text{cal}/\text{cm}^2 \text{ sec}$) (Korgen et al., 1971). The high heat flow of the margin continues throughout the accretionary complex and creates prime conditions for cooking organic matter and generating thermogenic methane. These high thermal properties and

high pressures of the Cascadia accretionary zone supply large quantities of thermogenic methane to south Hydrate Ridge, as seen within Horizon A.

HORIZON A

One of the main gas migration pathways is a stratigraphic horizon identified as Horizon A (Tréhu et al., 2004a). Horizon A was first identified from initial 3D seismic surveying conducted in 2000, where it appears as a high-amplitude reflection with a polarity opposite that of the seafloor. The reverse polarity and high amplitude implied a free-gas rich interval, but details from seismic reflections were limited. Horizon A was further investigated by drilling during Leg 204 in 2002. Logs at Sites 1245, 1247, 1248, 1249 and 1250 sampled Horizon A using standard LWD tools and cores. Cores from these sites indicated that Horizon A is composed of multiple coarse-grained, ash-rich turbidite beds that are roughly 5cm in thickness that combine into a total interval thickness of between 2 and 4 m (figure 29) (Tréhu et al., 2004b). The inter-layered ash-rich turbidite beds are dominated by silt and sand sized particles that are anomalous compared to the overlying clay-dominated sediment. The large grain size in Horizon A elevates the layer's permeability. The bulk density and porosity measurements indicated homogeneity within Horizon A (figure 29). The low density, high porosity, and coarse-grained nature of the ash layers within the turbidite beds that comprise Horizon A suggest that it has a high permeability and thus is an excellent conduit for methane transportation.

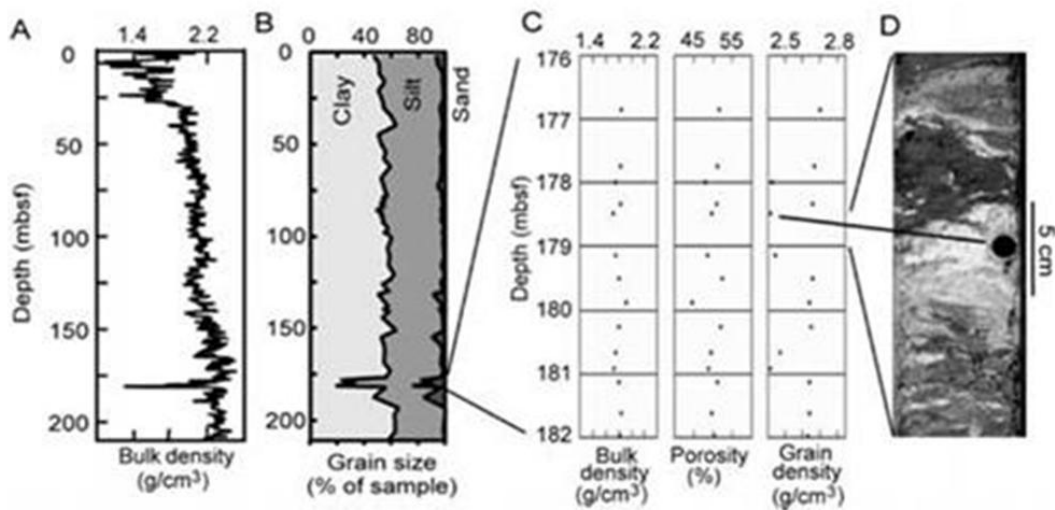


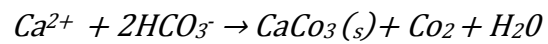
Figure 29: Bulk Density (A) and grain size (B) for Site 1245, with moisture and density measurements for Horizon A (C) and core image showing ash-rich layers of Horizon A (D) (reprinted with permission from Tréhu et al., 2004b).

The location of Horizon A further suggests that it is the main stratigraphic conduit for methane to reach the summit of south Hydrate Ridge. Horizon A dips north and shallows directly beneath the summit where active venting and gas hydrate formation are observed (figure 26). The turbidite beds of Horizon A intersect the BSR and enter the GHSZ along the western flank of the ridge near drill sites 1247 and also directly below the seafloor's authigenic carbonate pinnacle (figure 30). The pinnacle is thought to be a remnant of previous active seafloor venting at this site along a slightly different migration pathway than the current system. Free gas likely migrated to the shallow subsurface along the porous Horizon A and followed vertical structural pathways to the seafloor to form the authigenic carbonate pinnacle above the main source of gas. Carbonate precipitation is a product of the anaerobic oxidation of methane. The pore water contains

sulfate which, when oxidized, releases bicarbonate and hydrogen sulfide (Karaca et al., 2010):



During the anaerobic oxidation of methane, inorganic carbon is produced and alkalinity increases, which allows for authigenic carbonate to precipitate (Karaca et al., 2010):



The presence of the pinnacle directly above the intersection of Horizon A with the GHSZ suggests that methane migrated from Horizon A, oxidized, and precipitated authigenic carbonate at the seafloor.

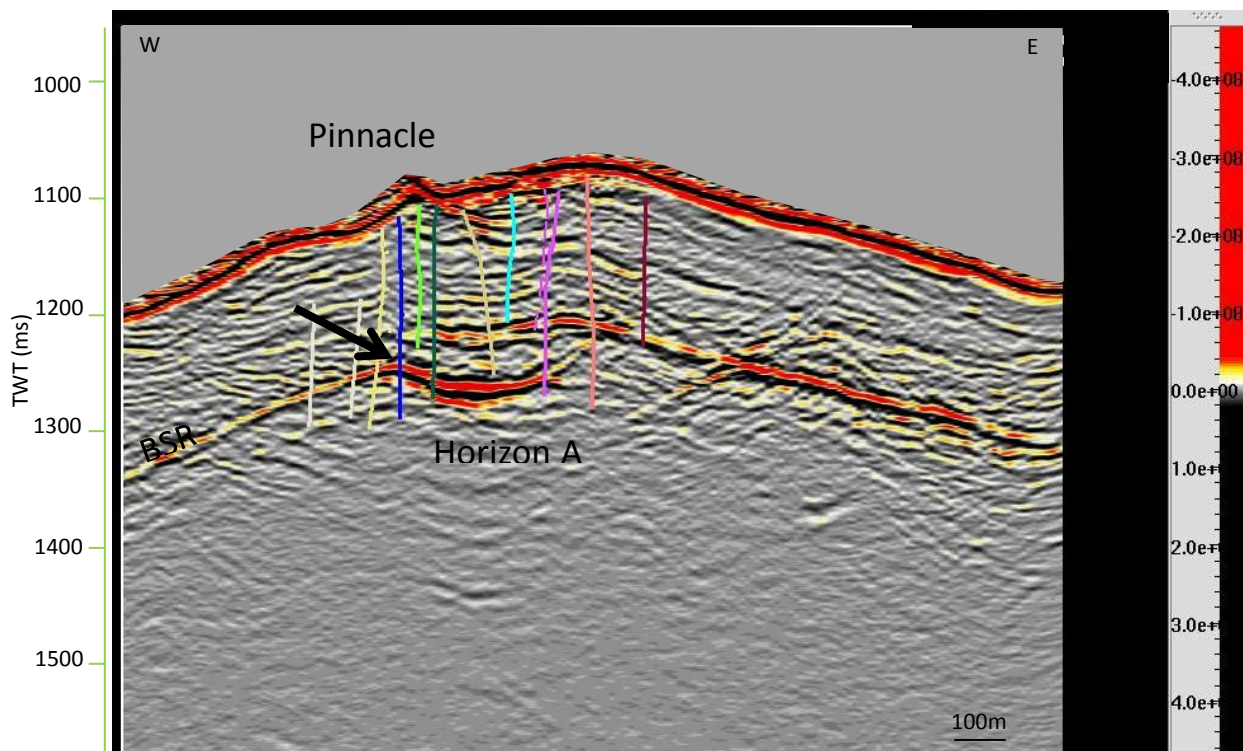


Figure 30: Crossline 584, with an arrow showing Horizon A entering the GHSZ (the base of which is the BSR) directly beneath the carbonate pinnacle.

Tréhu et al. (2004b) calculated gas saturations along Horizon A using density logs and shipboard porosity and grain density measurements, and found 50-90% gas saturation in the pore-space (figure 28). The bright, negative amplitudes of Horizon A, observed on the HR3D08 seismic data, correspond to these high gas saturations beneath the summit. The data acquired in the 2008 3D survey show for the down-dip continuation of Horizon A to the north for the first time. Horizon A to the north leads through a low-amplitude zone that transitions into a second set of similar amplitudes imaged on the down-dip, northern flank of Horizon A (figure 27). I believe that in addition to the highly saturated gas zone near the summit, Horizon A transitions into a second homogeneous zone of high

gas saturations at the northern most region of the survey, in the saddle between north and south Hydrate Ridge.

DISCUSSION

The log and core data from ODP Leg 204 indicate that Horizon A is a stratigraphically homogenous layer dominated by silt and sand size grains. Under these conditions, gas should be unhindered to migrate up-dip; however the amplitude extractions show two distinct zones of interpreted high gas saturations. Two zones of gas could be explained by stratigraphic or structural controls, or baric conditions. I am disinclined to interpret the zones as two separate stratigraphic accumulations of gas because the log and core data indicate that Horizon A is a porous, homogeneous layer and therefore an excellent conduit for gas. It is similarly unlikely that the zones are two structurally-separated gas accumulations because the seismic reflection of Horizon A is continuous with no evidence for cross cutting faults or traps.

I interpret the northern gas pocket as the source for the gas feeding the venting and hydrate formation at the southern summit of south Hydrate Ridge. The origin of this accumulation is unclear, however I expect it comes from further north (past the limit of the seismic survey) or from a deeper source yet to be imaged. Presumably, the gas accumulated in the north and accumulated prior to up-dip migration along Horizon A to the summit. The continuous compressional forces generated from the Cascadia subduction and accretionary margin result in numerous earthquakes or stress related events within the region. Seismic events like these could be responsible for triggering the intermittent mass migration of gas along Horizon A and produce the regional localization of gas accumulations along Horizon A.

The long term ODP monitoring sites at northern Hydrate Ridge documented thermal evidence for pulses of warm methane movement along a fault occurring at yearlong or more intervals (Tryon et al., 1999). Davis et al. (1995) suggest that these longer term fluctuations are tectonically driven. I believe that similar tectonically driven fluctuations occur at southern Hydrate Ridge as gas expels from the gas pocket on the northern flank to the summit. Future long-term monitoring stations on the southern ridge could provide evidence for episodic venting.

CONCLUSIONS

The composition, location, and geochemistry of Horizon A indicate that it is a potential high flux gas conduit carrying methane from depth to the GHSZ beneath the summit of south Hydrate Ridge. The homogeneity of the grain size and ash composition within Horizon A suggests that fluids could move through the pore-space unhindered by internal or lateral traps. The high gas saturations and gas compositions sampled from Horizon A indicate that thermogenic methane is being transported within the pore-space to the GHSZ. The bright negative amplitudes along Horizon A, beneath the summit, agree with the sampled gas saturations, however down dip to the north, a second set of high amplitudes is observed for the first time. These have not been drilled. I believe that Horizon A is a single, homogenous conduit and these amplitudes represent similar accumulations of gas within Horizon A as seen at the summit but are at an early phase of migration up to the south summit.

There is not sufficient evidence to assume that heterogeneity creates the two gas accumulations through lateral or internal traps, therefore I conclude that the reservoir is intermittently supplied from the down-dip location to the north. Possible methods for the

intermittent gas flux may include tectonic activity, such as fault reactivation or energy discharged through earthquakes and stress release events such as aseismic creep or slow-slip seismic events. This mechanism proposes that the gas at the summit originated in the pocket on the northern flank and expelled in a major migration event to the summit of the ridge. Presumably, this process repeats as gas continues to migrate to the northern flank of Horizon A and releases when another stress event occurs, but will require additional long-term fluid flow monitoring efforts to confirm that this indeed is the mechanism responsible for these observations.

Chapter 4: Venting Processes and Hydrate Formation

The previous chapter's primary focus was the generation and presence of methane in the stratigraphic layer, Horizon A. The following chapter will address the processes affecting the methane after reaching Horizon A, including the creation of structural migration pathways, gas hydrate formation, and active seafloor venting at the summit of south Hydrate Ridge. I interpret two possible primary migration fault-related features in the HR3D08 seismic reflection data volume, a set of thrust faults on the northern flank of the ridge and a densely-spaced network of shallow vertical fractures beneath the summit of south Hydrate Ridge.

Active venting of methane at ODP Sites 1248-1250 support rapid growth of gas hydrate ($\sim 10^2 \text{ mol CH}_4 \text{ m}^{-2} \text{ year}^{-1}$) observed at and near the seafloor (Torres et al., 2004). Torres et al. (2004) concluded through numerical modeling of south Hydrate Ridge's fluid flow regimen that vertical transportation of methane in the free gas phase through the GHSZ is necessary to produce the observed hydrate deposits and growth rates. Tréhu et al. (2004a) demonstrated that the fluid pressures within Horizon A are sufficient to sustain steady-state gas migration to the seafloor through vertical fractures or faults.

FAULTS

Examining the HR3D08 reflection data volume identified multiple vertical displacements of reflectors (figures 31 and 32). These discontinuities occur in N-S trends that dip West, with typical vertical displacements greater than 10ms. Quantifying the extent of the features' depths is difficult due to the decrease of seismic resolution below 400msbsf, however they appear at Horizon A and deeper. The displacements are also

associated with isolated incidents of bright, negative seismic amplitudes less than -2.0×10^8 .

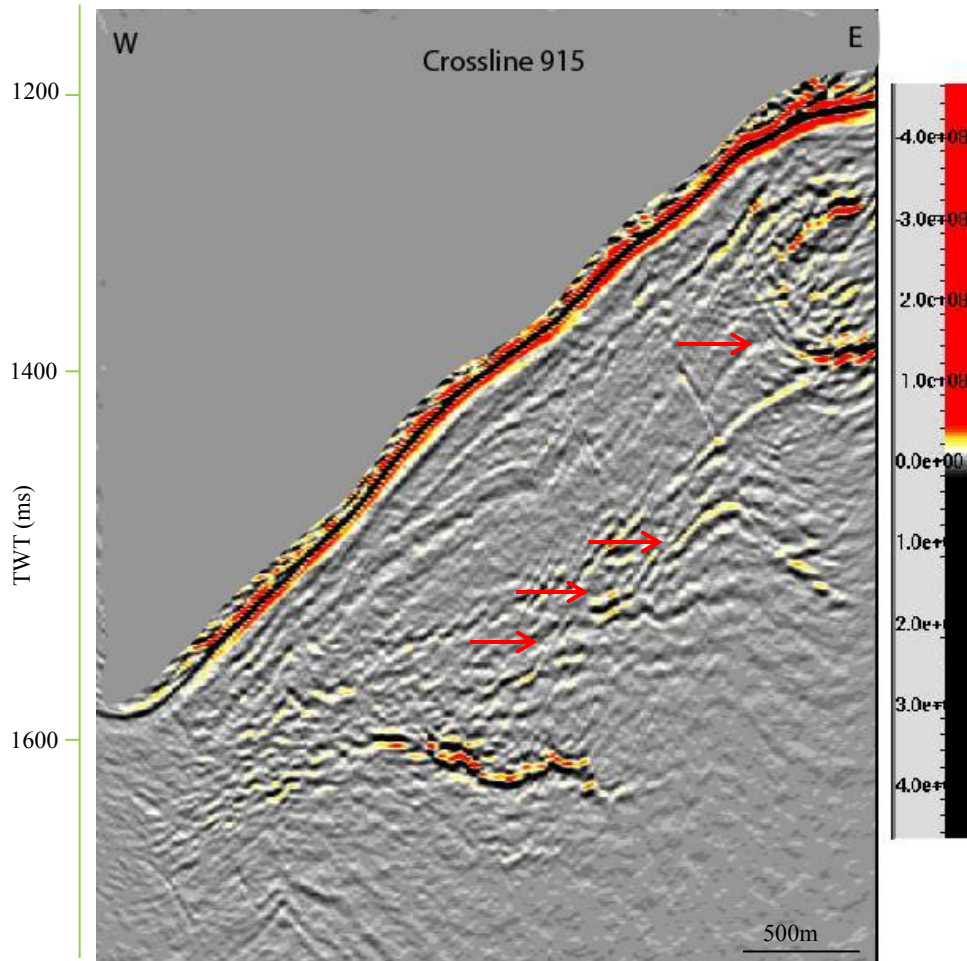


Figure 31: Examples of vertical and horizontal discontinuities along crossline 915.

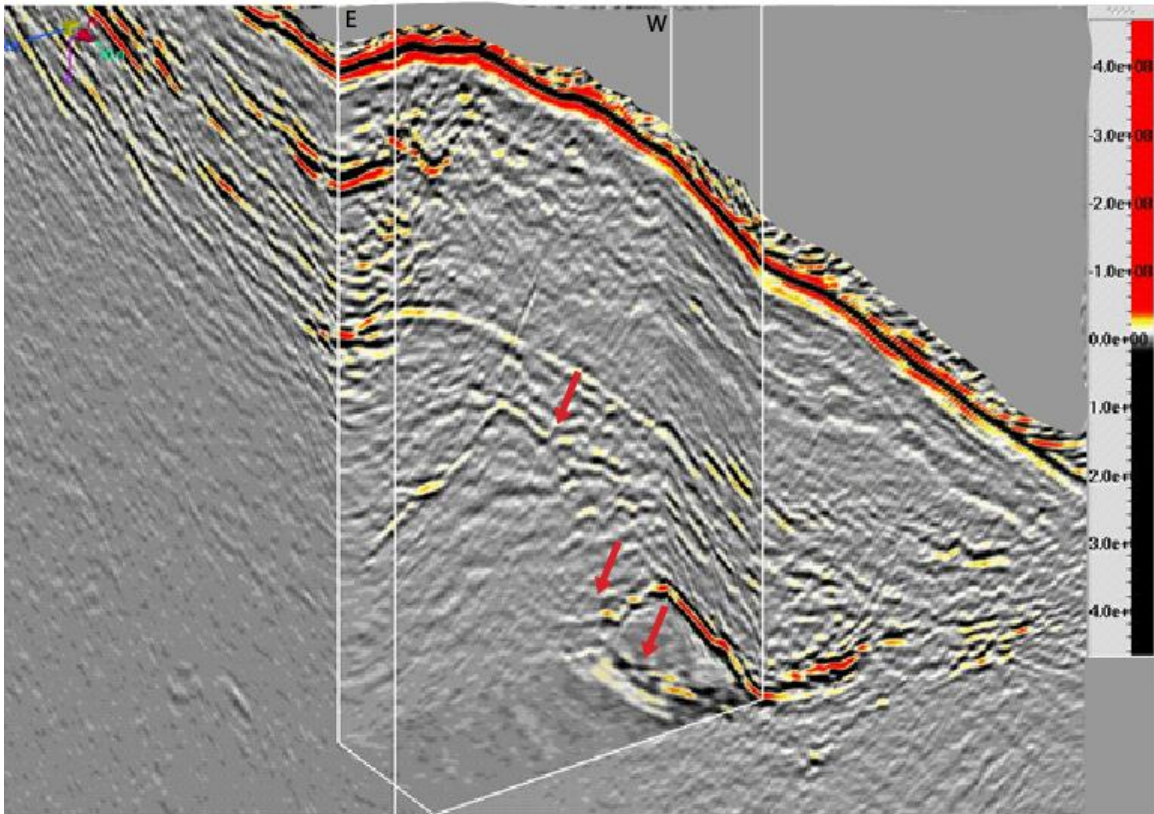


Figure 32: 3D view of vertically lined displacements.

I interpret the displacements as faults if they conform to the following criteria; 1) they have a minimum vertical displacement of 3ms 2) they are continuous along strike for a minimum of 15 crosslines (187.5m) and 3) they are continuous along dip for a minimum of 10 inlines (125m). These criteria were determined to distinguish between geological features and artificial noise from the acquisition or processing. Figures 33 and 34 display examples of the interpreted major faults in a crossline and a 3D cube view. These faults trend N-S and have dips typically less than 50° . They are not restricted to any specific depth, but are interpreted to occur predominately along the flanks of the southern ridge. Minor normal faults, with lengths less than 100m, exist predominately

along the far edges of the eastern and western flanks of the southern ridge. I do not believe the normal faults play a significant role in the primary fluid migration system, as they do not directly interact with the summit features or the major gas bearing layer, Horizon A.

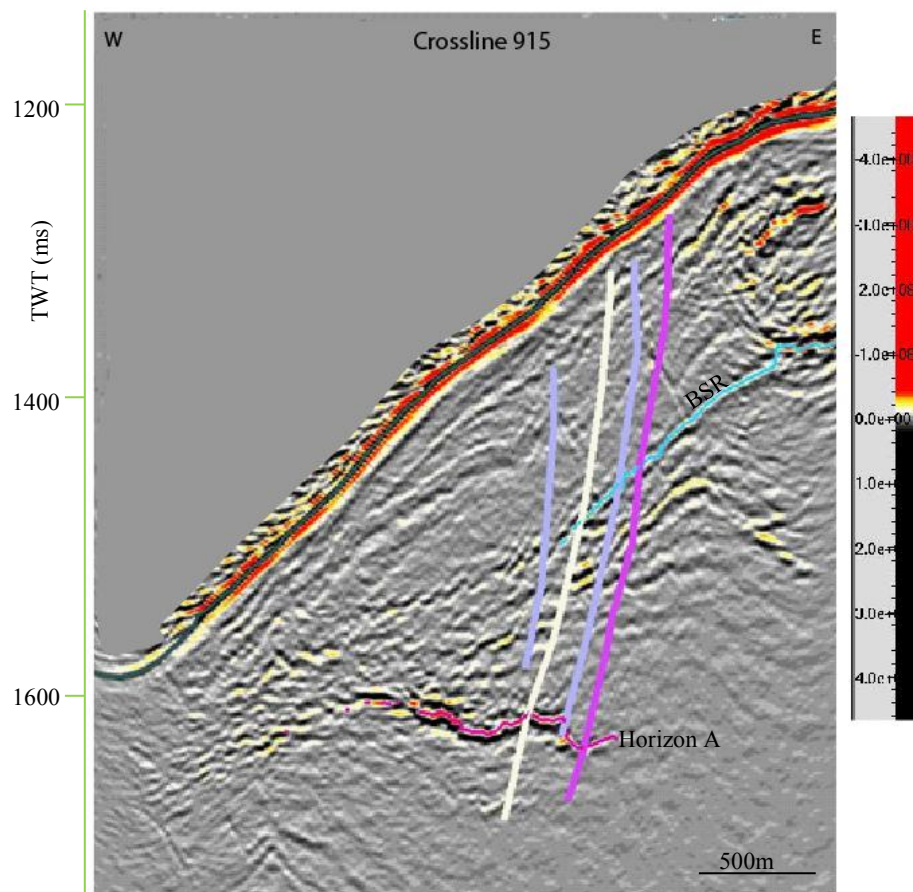


Figure 33: Crossline 915, example of a selection of interpreted thrust faults.

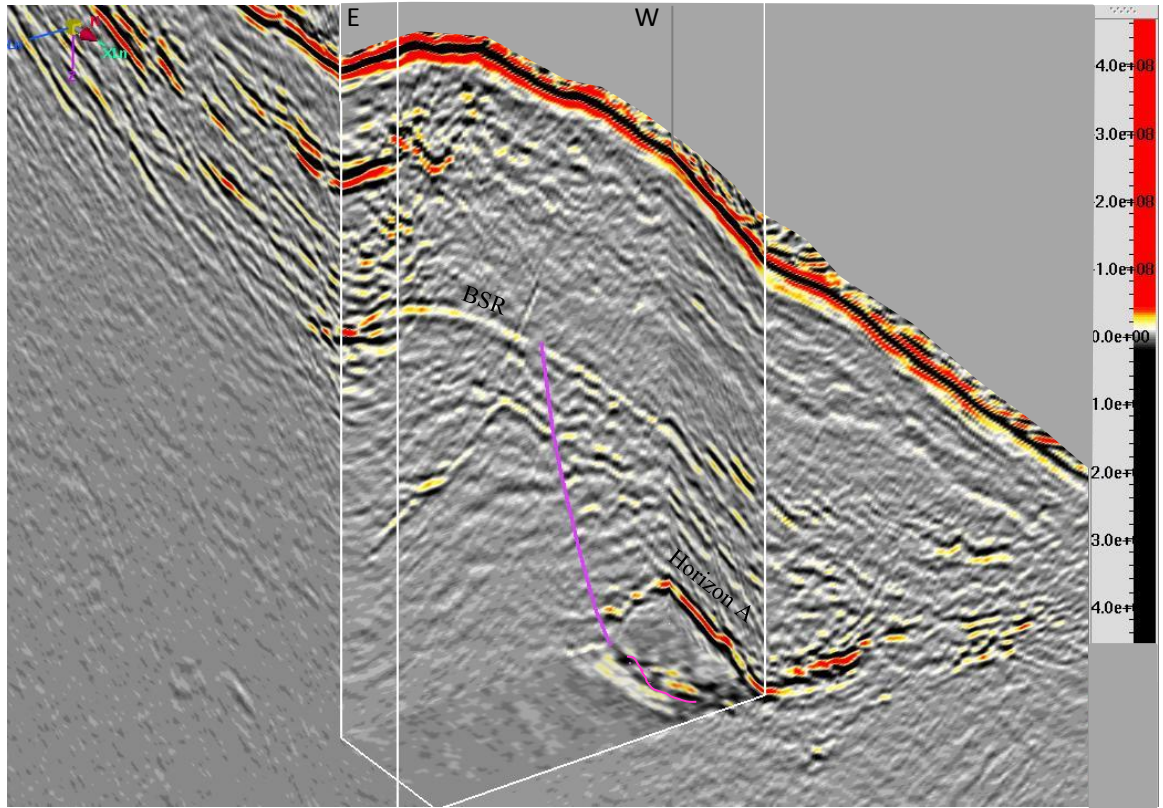


Figure 34: Example of vertically lined displacements, interpreted as a thrust fault in 3D cube view.

The major faults are interpreted as thrust faults, as the reflections on the hanging walls are up-dip compared to those along the foot wall (figure 33). Three major thrusts are along the northern flank of the ridge, near the saddle between north and south Hydrate Ridge (figure 35). These are estimated at 750m-1000m in length. Four of the thrusts occur on the north-eastern flank of the ridge, roughly 1500m from the summit. These are estimated at 250m-500m in length. A set of four thrusts, roughly 100m-250m in length, are interpreted on the southeastern flank, roughly 600m from the summit. The longest of the thrust faults interpreted, roughly 2500m in length, is on the northeastern flank of the ridge, and trends along strike of the southern ridge, NE-SW. Previous surveys have

suggested a major seaward-verging regional thrust fault beneath Horizon A that was responsible for the uplift of Hydrate Ridge (Chevallier et al., 2006). This feature was not clearly imaged in the new 2008 3D seismic survey, possibly due to the loss of signal and resolution deeper than Horizon A.

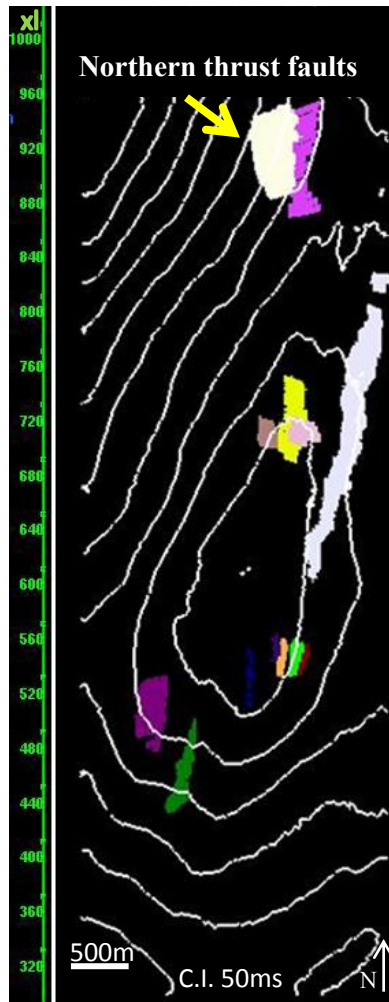


Figure 35: Map of the major interpreted thrust faults which are primarily located on the flanks of south Hydrate Ridge. The three northern most faults may play a role in supplying deeply sourced thermogenic methane to the system.

I believe that the longer and shallower faults, those on the northern flank and the SW-NE trending fault along the northeastern flank are a result of the regional compressional forces along the Cascadia convergent margin. These are longer than the other observed thrusts by 250m-1500m and extend to greater depths, including penetrating Horizon A. The smaller thrust faults are located closer to the summit and have steeper dips than the regional thrusts. These are likely products of localized compressional forces. Local tensional forces that occur naturally along the far eastern and western flanks of the ridge likely produce the minor normal faults that were not interpreted in detail in this volume.

NATURAL HYDRAULIC FRACTURING & HYDRATE FORMATION

In the HR3D08 seismic volume, the shallow subsurface (less than 50msbsf) contain multiple near-vertical (greater than 70° dips) discontinuities in horizontal reflectors. These discontinuities include horizontal displacement along a reflector, abrupt truncation of bright amplitudes, and vertical blank-out zones where the amplitudes are dim. Typically, the vertical displacements of these features are less than 10ms. The shallow nature of the survey can result in noise contamination from the unconsolidated sediments near the surface, which may relate to the discontinuities. Therefore it is important to identify guidelines for distinguishing between geological features and artificial noise.

I interpret the vertical discontinuities as natural fracture networks if they conform to the following criteria; 1) they are continuous along strike for a minimum of 15 lines 2) they are continuous along dip for a minimum of 10 lines and 3) they have a minimum lateral displacement of 3m. Although some of the observed discontinuities had vertical

offset, no vertical displacement restrictions were applied to these criteria because natural hydraulic fractures do not require vertical displacement. The observed discontinuities are not likely caused by single individual fractures, which may only be centimeters in thickness and unresolvable in seismic, but from multiple fractures forming an interconnected network several meters thick. The interpreted fractures on the seismic represent these numerous cracks and fractures which have joined together. Figures 36 and 37 are examples of the interpreted vertical fractures in a 3D cube view. Each identified feature can be tracked in the time slices as well as the cross sections. Interpreting the data identified 30 fracture network features in the shallow subsurface at and around the summit of south Hydrate Ridge, roughly trending N-S along the strike of the ridge. The strike lengths of the fractures vary from 50m to 600m, with no fractures the same; however the typical length observed was 300m.

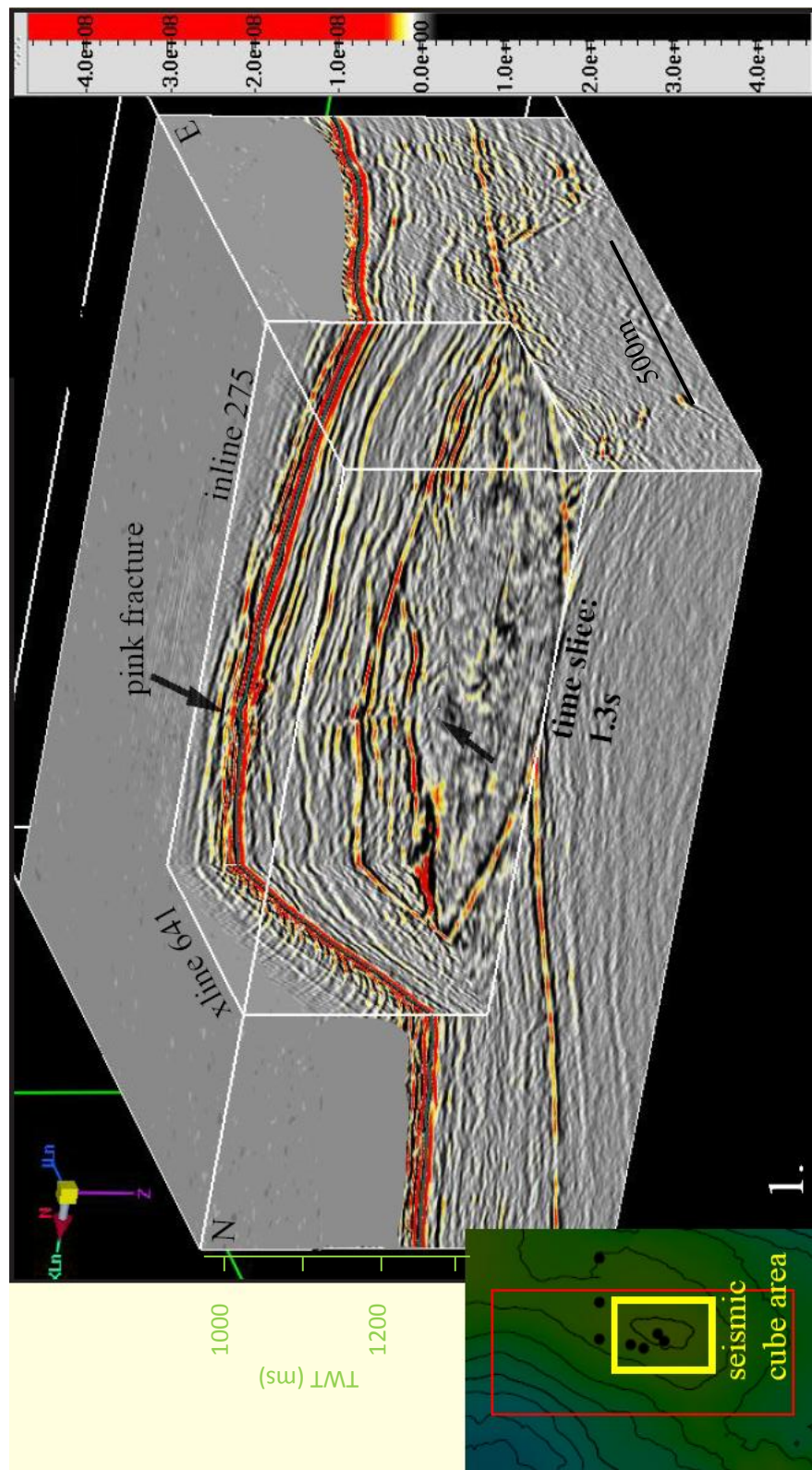


Figure 36: Example of an uninterpreted fracture (pink fracture) in a 3D cube volume

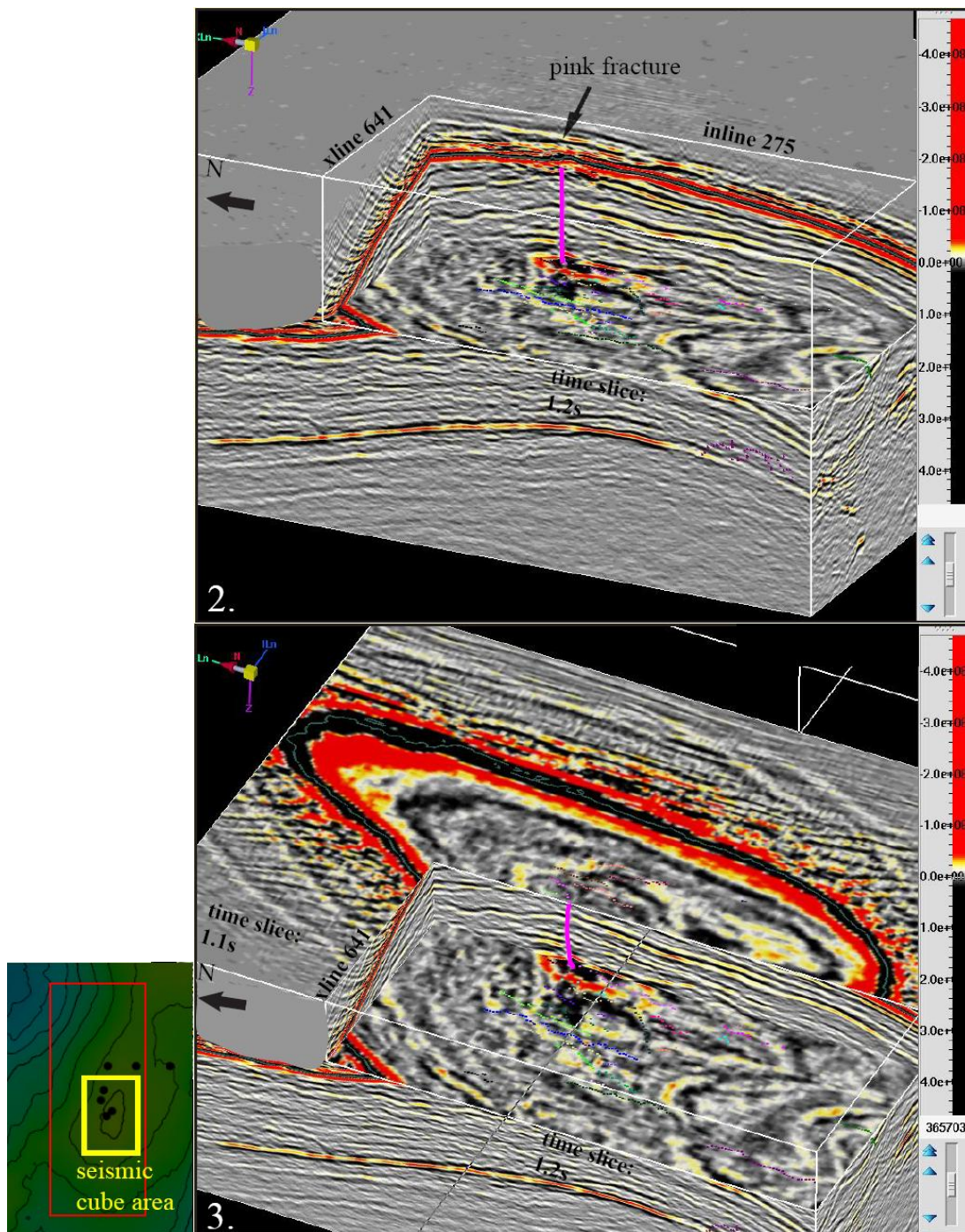


Figure 37: Example of the interpreted pink fracture network in a 3D cube view.

The fractures are further broken into two groups, those that are limited to within the gas hydrate stability zone and those that continue to penetrate Horizon A. Figure 38 displays a selection of the summit fractures where 9 of the fractures terminate at or just below the BSR. The remaining 6 fractures extend to Horizon A and appear to end at or just below Horizon A. The loss of resolution below Horizon A, due to signal damping and attenuation creates ambiguity in determining the depth of the second group of fractures.

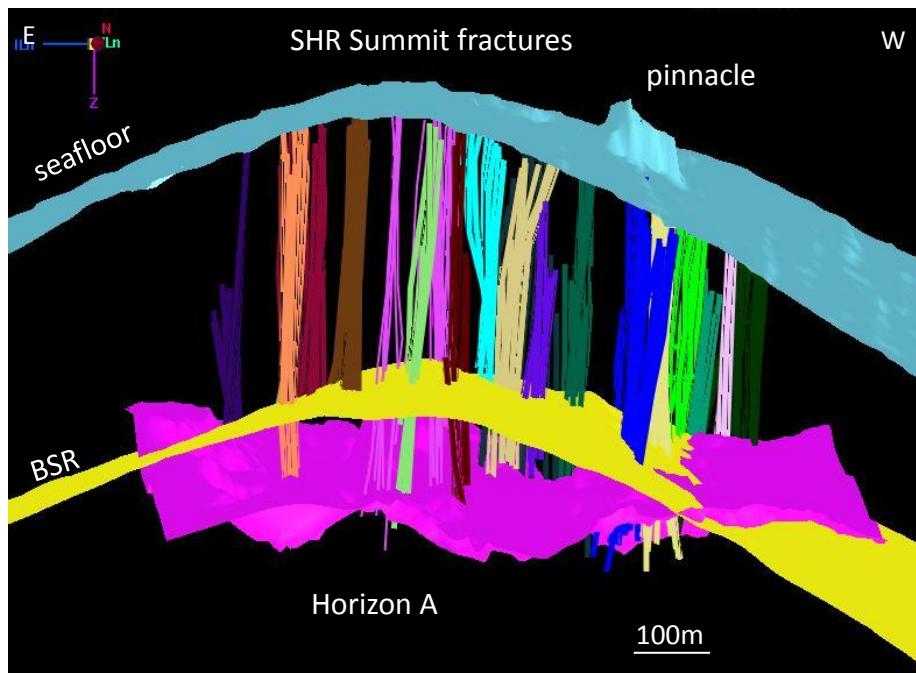


Figure 38: Clipped perspective view, looking South, of a selection of summit fractures, with each color corresponding to an individual fracture. 9 of the fractures shown terminate at or just below the BSR, while only 6 penetrate Horizon A.

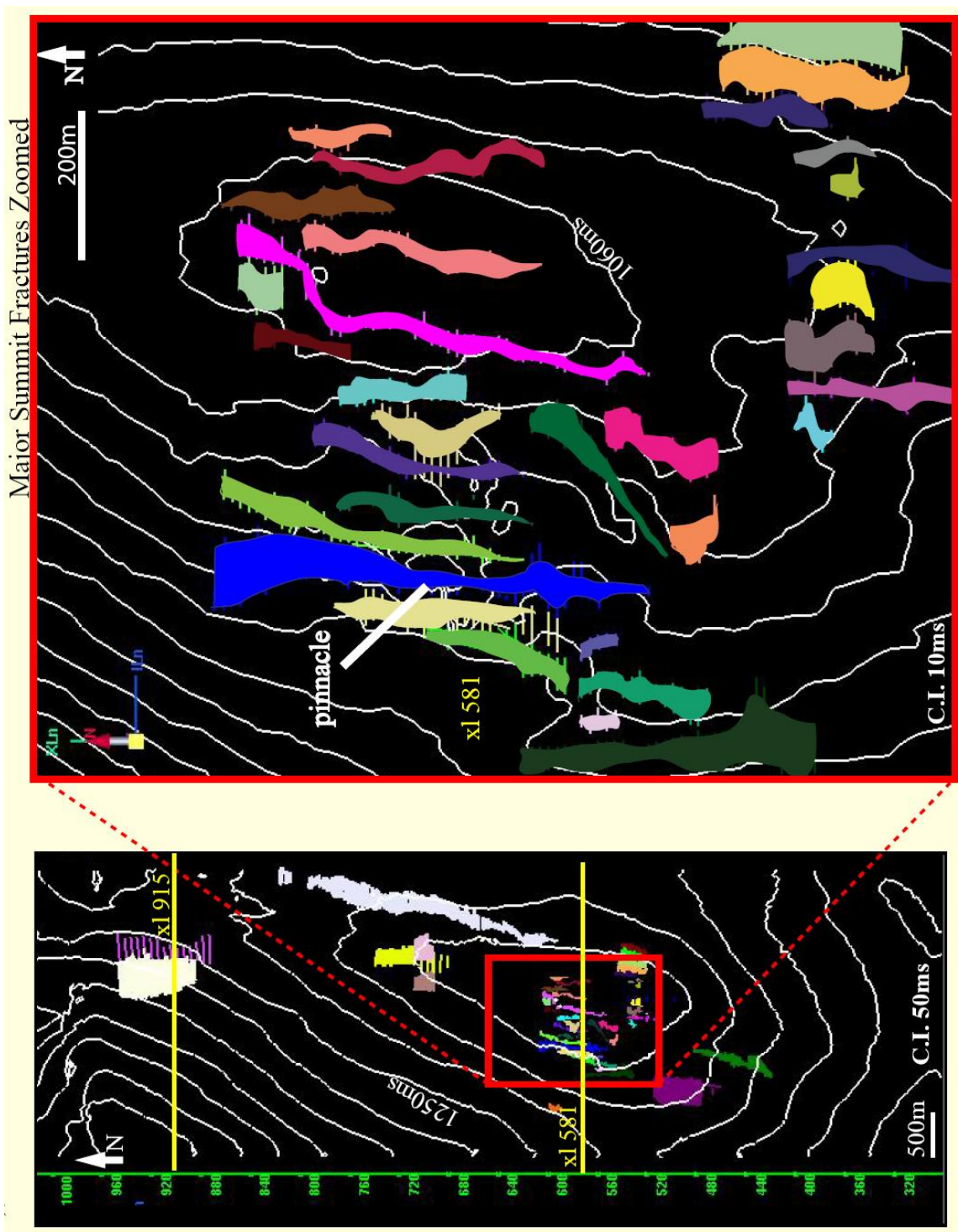


Figure 39: Zoomed-in view of the interpreted fracture networks located along the summit of south Hydrate Ridge.

The fractures may develop through the process of natural hydraulic fracturing. As explained earlier, natural hydraulic fractures occur when pore-fluid pressures approach or exceed lithostatic pressures and the tensile strength of the surrounding sediments. They are prevalent below the summit of south Hydrate Ridge, which is consistent with the over-pressured gas samples from the ODP drilling sites at the summit. The episodic process of natural hydraulic fracturing and collapse results in numerous propagations with different geometries (Luo and Vasseur, 2004), which is consistent with the variations in depths, lengths, and lateral continuity of the interpreted fractures.

DISCUSSION

Fractures have often been inferred in gas hydrate environments, such as the Blake Ridge, (Taylor et al., 1999; and Flemings et al., 2003) Cascadia margin (Torres et al., 2004; Tréhu et al., 2004b; and Tréhu et al., 2006) and the mid-Norwegian margin (Hustoft et al., 2007), as mechanisms for increasing porosity and migrating fluids. Individual fractures in these settings are millimeter to centimeters in width, and therefore unresolvable through seismic reflection imaging. A compact network of individual vertical fractures could span several meters in width and therefore might be detectable through high resolution 3D seismic imaging. X-ray images of core samples from the Indian national gas hydrate program detected hydrate-filled vertical fractures (figure 40) (Collett et al., 2006). The cores indicate that the fractures form a closely-spaced (centimeters in scale) network of hydrate-filled cracks and nodes. LWD results and seismic impedance volumes in the East Casey fault zone at Keathley Canyon of the Gulf of Mexico also showed networks of hydrate-filled fractures within the GHSZ (Dev and McMechan, 2010). Similar fracture networks beneath the summit of south Hydrate Ridge

likely cause the vertical discontinuities that were interpreted on the HR3D08 seismic volume.

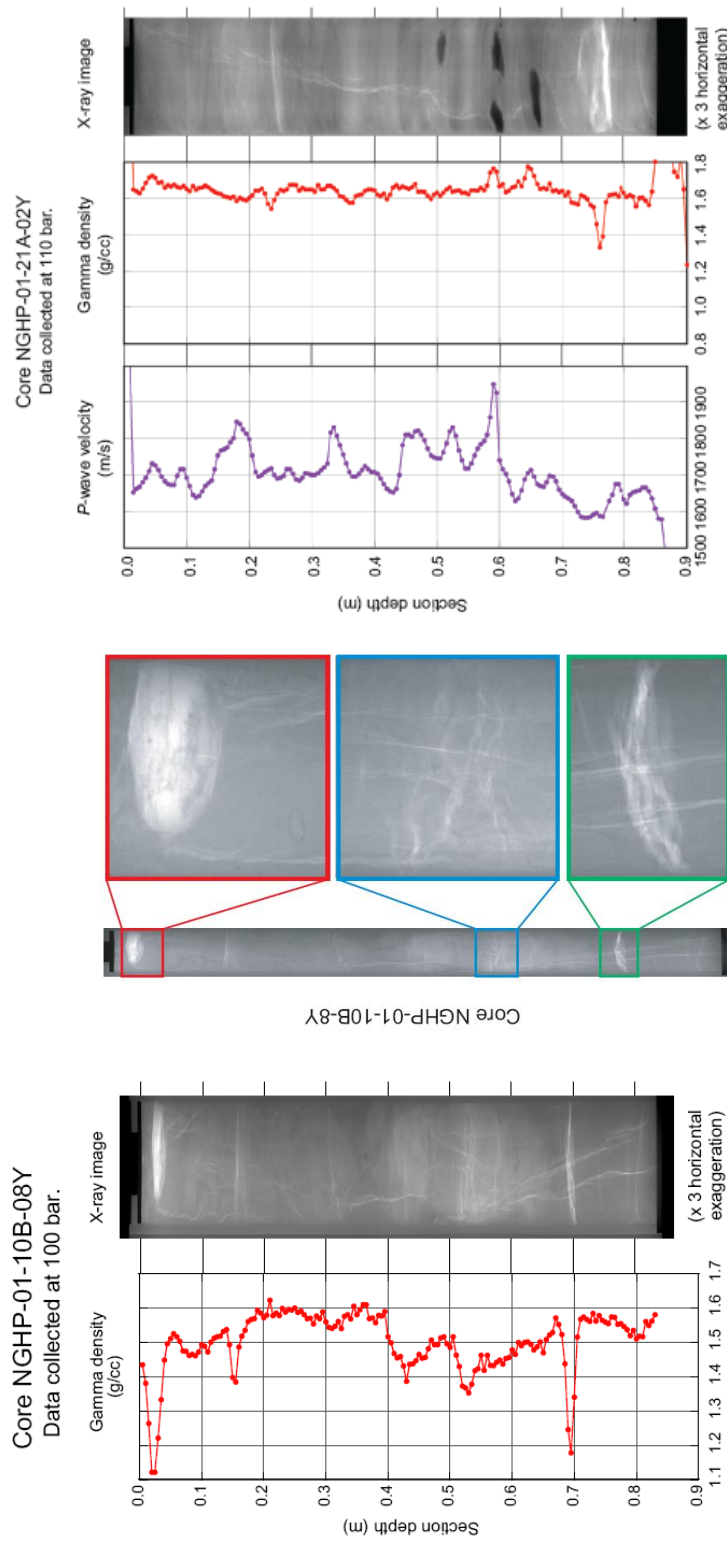


Figure 40: (left) Gamma density measurements and X-ray image of 4inch core from offshore India where hydrate was imaged within vertical fractures. (center) X-ray image of core from offshore India where gas hydrate nodes were imaged as well as gas hydrate within vertical fractures (right) P-wave velocity, gamma density and X-ray image of core sampled from offshore India. Notice the network of vertical, hydrate-filled fractures imaged by the core X-ray (modified from Collett, 2006).

The fracture networks interpreted beneath the summit of south Hydrate Ridge could be responsible for the active methane venting seen on the seafloor. Nine of the fractures penetrate Horizon A, a well-documented gas rich stratigraphic conduit. These fractures would provide access for the methane in Horizon A to migrate into the GHSZ. Overtime, gas hydrate would form within the fractures, forming similar features as the hydrate-filled veins from offshore India (figure 40). The hydrate-filled fracture networks are resolvable within the GHSZ, where the gas hydrate supports the walls of the fractures. The features interpreted in the HR3D08 volume that truncate at the BSR (figure 38) are potentially these hydrate-filled fractures. Below the GHSZ, the fractures are collapsed or unresolvable because there is no gas hydrate displacing the sediments. The interpretations of the two sets of fracture networks will be described in further detail in Chapter 5.

CONCLUSIONS

Two structural features were interpreted within the HR3D08 seismic volume, thrust faults and near-vertical fractures. The thrust faults occur on the flanks of the ridge, striking in the N-S direction. These faults may play a role in bringing thermogenic methane from greater depths to the shallow subsurface and Horizon A. They do not appear to directly feed the active seafloor vents at the summit of south Hydrate Ridge, and likely introduce methane into the shallow sub-surface where gas hydrate forms.

I believe that the near-vertical fractures at the southern summit of Hydrate Ridge are formed through hydraulic fracturing as gas beneath the GHSZ reaches near-lithostatic pressures. Offshore India provides an analogue for hydraulic fracturing in gas hydrate

systems, where X-ray core samples show complex networks of vertical, hydrate-filled fractures. The fracture networks observed in India represent the fracture interpretations on the HR3D08 data volume. Six of the interpreted fracture networks penetrate Horizon A and could be transporting methane into the GHSZ and to the seafloor vents at the summit.

Chapter 5: South Hydrate Ridge Migration System Discussion

I concluded that the fluid migration system of south Hydrate Ridge is predominately controlled by the vertical fractures at the ridge's summit. I hypothesize that the formation of fracture networks is a factor of methane migration to the GHSZ and gas hydrate development. The presences of bright amplitudes along the BSR and Horizon A have been discussed as well as the interpretation of both faults and vertical fractures. This chapter will discuss and support the previous claim that the fractures act as conduits to supply methane to the surface by examining the relationships between the seismic stratigraphy and the interpreted structures.

FRACTURE DEVELOPMENT

The data suggest that the evolution and development of gas conduits through the GHSZ is a dynamic process that changes overtime. Gas hydrate is known to form in massive deposits within the upper 30mbsf at south Hydrate Ridge (Torres et al., 2004) and I believe that the process of hydrate formation indirectly instigates the propagation of fractures throughout the shallow subsurface by trapping free methane and increasing pore-fluid pressures. The cycle of pressure buildup and release makes the timing of natural fracture formation difficult to determine, however by examining the geometries of the fracture networks I am able to qualify which may be active conduits and which may be inactive.

The gas likely migrates from depth along the primary thrust faults imaged along the flanks of the ridge. The faults on the northern flank of the ridge, near the saddle between the southern and northern ridges of Hydrate Ridge, likely play an important role in gas migration. They penetrate the deepest of all the features interpreted, roughly

400msbsf, and cross cut the GHSZ and Horizon A at its deeper extent, 1800msbsl, therefore they are potential candidates for bringing thermogenic methane up from depth.

As the gas migrates to the GHSZ, hydrate precipitates within the pore-space of the unconsolidated sediments. Gas pressures beneath the GHSZ reach near-lithostatic pressures, initiating hydraulic fracturing in the sediments above. These fractures will propagate up from the source of the overpressure, Horizon A, and release gas into the GHSZ or reach the seafloor and release gas into the water column. The fluid pressures within a fracture will maintain its structure and prevent collapse. I presume the fluid in the fractures will eventually lead to hydrate crystallization within the fracture. Over time, the hydrate precipitation will block further gas from migrating along the fracture. The blockage of the active conduits will cause the gas pressures beneath the GHSZ to increase again until the process repeats itself and new fractures are formed. A study by Daigle and Dugan (2010) determined that the time frame for fracture development in hydrate rich environments is a factor of fluid-flow rates and permeability loss. Models involving fluid-flow rates and sediment ages concluded that fracture development due to increasing pore-pressures is feasible at Hydrate Ridge (Daigle and Dugan, 2010). The time frame for natural fracturing in the hydrate-saturated, coarse-grained layers of Hydrate Ridge was estimated to occur after 2000 years (Daigle and Dugan, 2011).

I propose that the episodic process of hydraulic fracturing is responsible for the two groups of fractures interpreted at the summit of south Hydrate Ridge. The fractures that extend from the seafloor down to Horizon A are thought to be the more recent and possibly active conduits feeding methane into the system. The fluid pressures from the migrating gas will maintain the walls of a fracture and keep it open. I interpret the second group of fractures, those that truncate at a shallower level, as older, inactive

conduits because there is no active fluid movement to maintain the walls of the fractures open beneath the GHSZ. These once supplied methane into the GHSZ system, however an inactive conduit that does not have sufficient gas or fluid pressure to maintain an open fracture will collapse. The fracture segments beneath the GHSZ collapse as the fracture collapses with loss of the internal fracture pressure. For this reason, fractures can be seismically imaged within the GHSZ because the structures are maintained by the hydrate filling. The fractures appear to truncate at the BSR because the remaining segment has collapsed and is no longer seismically present (figure 41).

The seafloor vents are being fed through the vertical fractures and change over time as the active fractures close and new fractures open. I suggest that the pink fracture network (figure 39) is the active conduit supplying the current gas seeps (figure 9) on the seafloor of south Hydrate Ridge because it provides a direct path from the gas rich Horizon A to the location of the seafloor seeps. The blue and green fractures (figure 39) are believed to have been the conduits that fed the formation of the carbonate pinnacle, because they intersect Horizon A and lead vertically to the seafloor location of the pinnacle. A long term supply of methane is needed to form the authigenic carbonate observed at the pinnacle, so presumably the blue and lime green fracture networks were active during this time. They still penetrate to Horizon A and may be involved in supplying gas into the GHSZ.

The network proposed for direct vertical migration differs from previously suggested migration pathways at south Hydrate Ridge. In the previous scenarios, it was proposed that the gas migrated into the GHSZ from Horizon A through a gas chimney beneath the carbonate pinnacle and then laterally through permeable stratigraphic layers to the seafloor vents (Tréhu et al., 2004b; Torres et al., 2004; Liu and Flemings, 2006).

The higher resolution of the 2008 seismic reflection data improved the detail of the shallow subsurface and led to the new interpretation of the vertical fractures described through this research. The fluid migration system may also involve lateral migration within the GHSZ as previously proposed, however I suggest that the primary mechanism for supplying methane from Horizon A to the seafloor vents is the vertical fracture networks interpreted at the summit.

The evidence for gas driven fracture networks at south Hydrate Ridge supports data from Blake Ridge, offshore Norway, and offshore Vancouver Island. At Blake Ridge, lithostatic gas pressures were proposed to dilate vertical fractures, which allowed for free gas to rapidly migrate through the GHSZ to the seafloor without converting to hydrate (Flemings et al., 2003). Similar results were inferred on the mid-Norwegian margin, where high gas pressures result in the generation of fractures to increase permeability through a GHSZ (Hustoft et al., 2007). Natural hydraulic fracturing was inferred in the hydrate rich environment of offshore Vancouver Island (Zühlsdoff and Spieß, 2004). It was proposed that focused fluid flow and high gas pressures instigated the development of the inferred fractures.

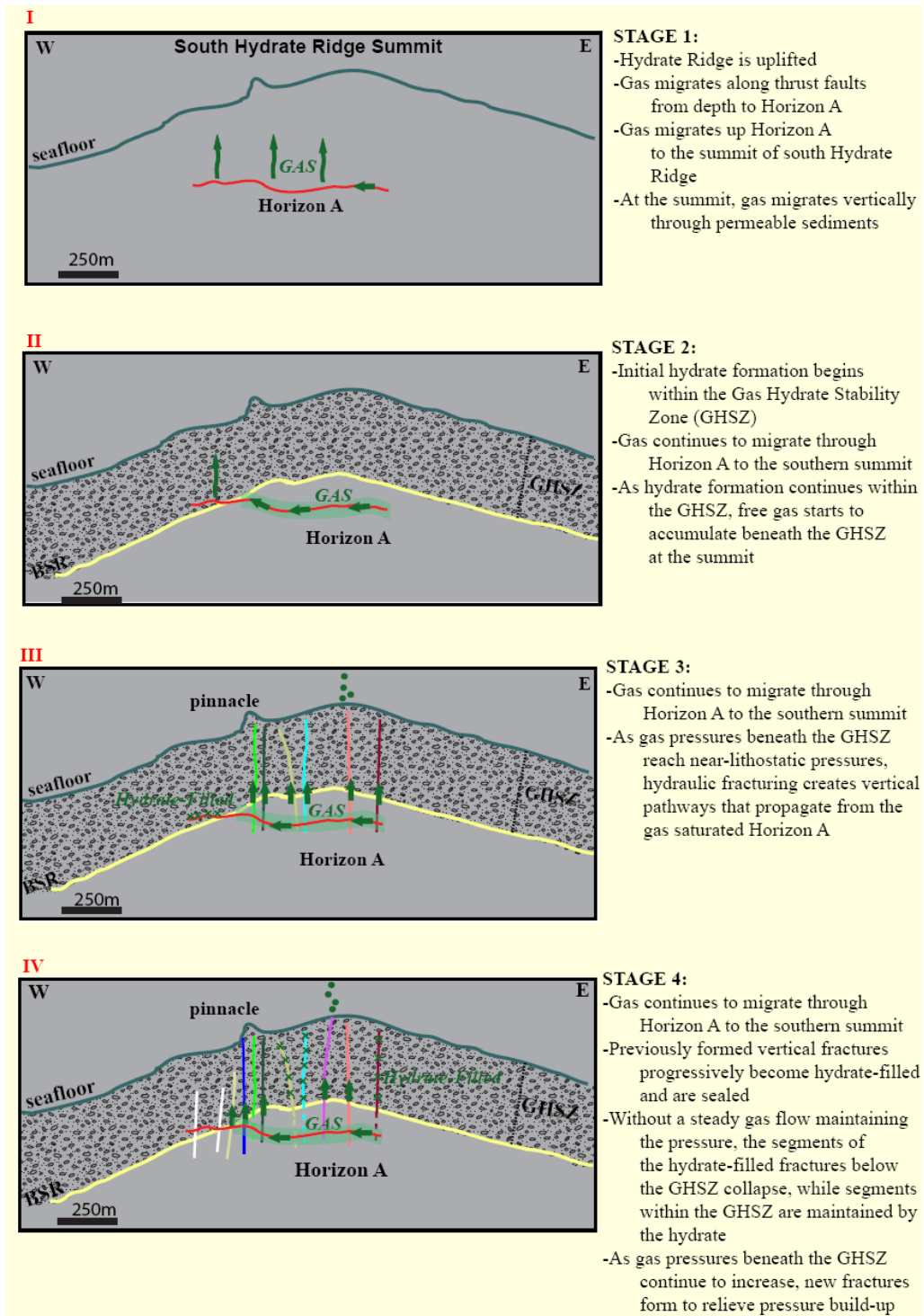


Figure 41: Fluid migration and fracture development process.

REFLECTION AMPLITUDE ANALYSIS

Variations in seismic reflection amplitudes extracted from the BSR coincide with mapped fractures at the summit and faults along the ridge's flanks (figure 27). Slight increases in amplitudes along the BSR occur at the summit, where the vertical fractures are prominent, however the brightest amplitudes are observed along the eastern flank (figure 27). These amplitudes do not directly coincide with the interpreted faults in that region. One explanation for these high amplitudes is coherent noise caused by the surrounding reflection interfaces of the same dip as the BSR constructively interfering with the BSR's amplitude.

Large amplitudes observed at from Horizon A provide a correlation of presumed gas accumulations and by inference, the presence of fractures. The strongest amplitudes of Horizon A, denoting the presence of free methane within the stratigraphy, are found along a 1,875m by 625m area directly beneath the summit where active methane seeps have been observed (figure 27). These bright amplitudes are bounded on both sides of the x m wide zone by fractures that penetrate Horizon A (figure 42). No strong correlation is observed between the fractures that are truncated at the BSR and the high amplitudes of Horizon A. This is consistent with the interpretation that these fracture segments are no longer in communication with Horizon A.

The presence of gas at the base of the deeper fractures supports our previous claim the active fractures are those that penetrate Horizon A. I assume the methane pooling in Horizon A increases the pore-fluid pressure and instigates hydraulic fracturing. The most prominent fractures networks that bound the gas in Horizon A are the pink, blue and lime green fracture shown in figures 43 and 44. The pink also cuts the seafloor at the location of active seeping, and therefore is likely the current active pathway

feeding the vent. The blue and lime green fractures do not cut the seafloor, however they are directly beneath the carbonate pinnacle and are assumed to have been the long sustained pathway that allowed methane to flow for a sufficiently long time to allow the pinnacle to grow to its large size. If these fractures are the main feeders to the pinnacle, they were also involved in shutting down the flow of methane to the pinnacle and causing it to cease. It is currently no longer actively growing. Although these two fractures no longer feed methane to the seafloor, they likely provide a pathway for methane from Horizon A into the GHSZ. Once in the GHSZ the methane could migrate laterally through porous layers or contribute to the formation of gas hydrate. Future seismic surveys over the saddle feature could determine the extent of the high amplitudes in Horizon A.

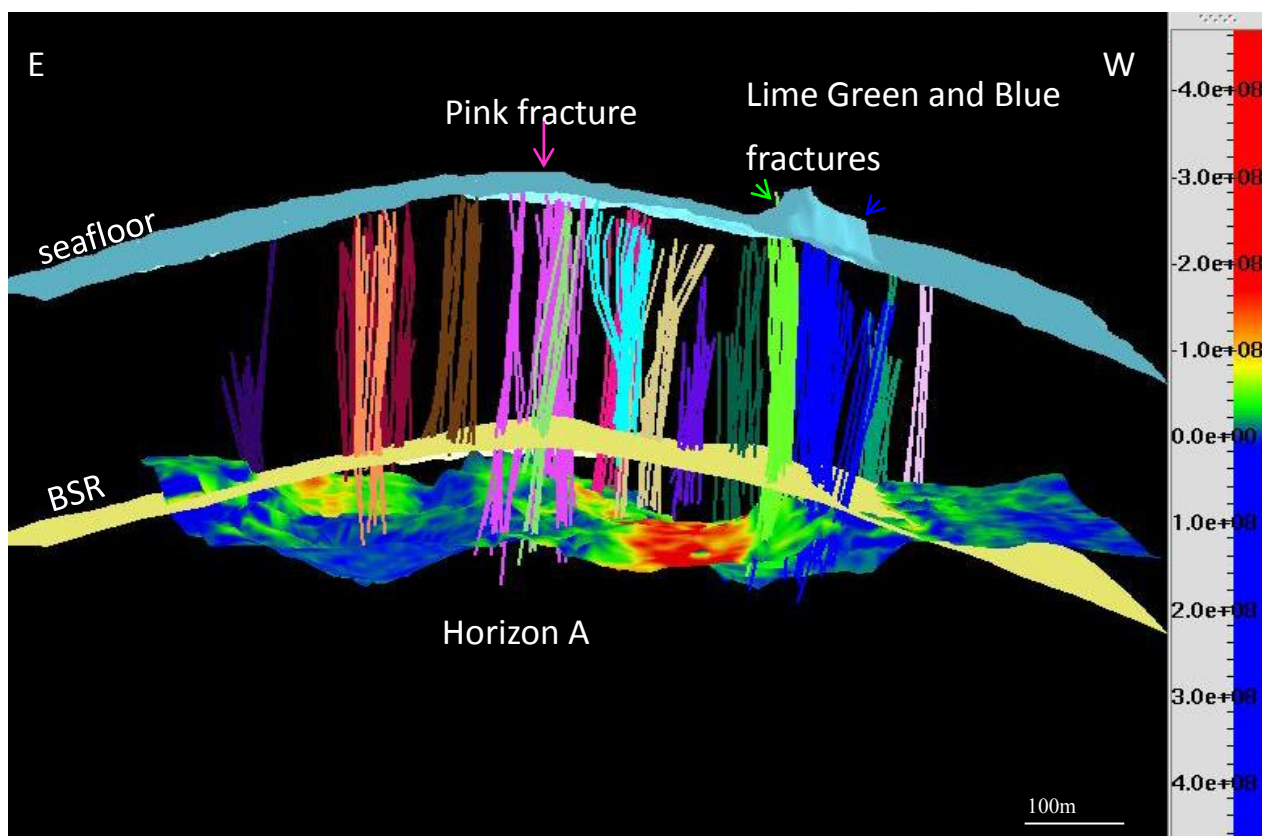


Figure 42: Clipped perspective view of a selection of summit fractures (looking south) with each color corresponding to an individual fracture. The fractures which penetrate Horizon A correspond to incidents of high amplitudes.

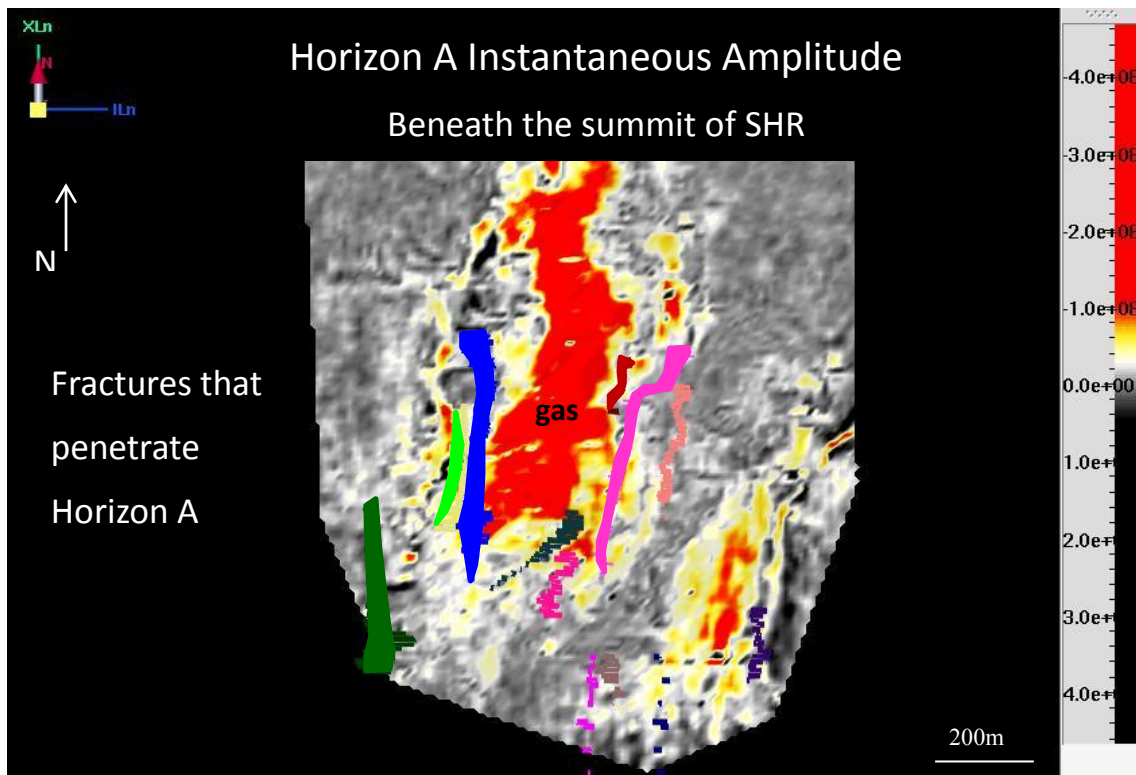


Figure 43: Map view of the fractures that penetrate Horizon A with respect to Horizon A's instantaneous amplitudes. Note how the blue, lime green and pink fractures bound the zone of highest amplitude where the greatest concentration of gas is assumed to be.

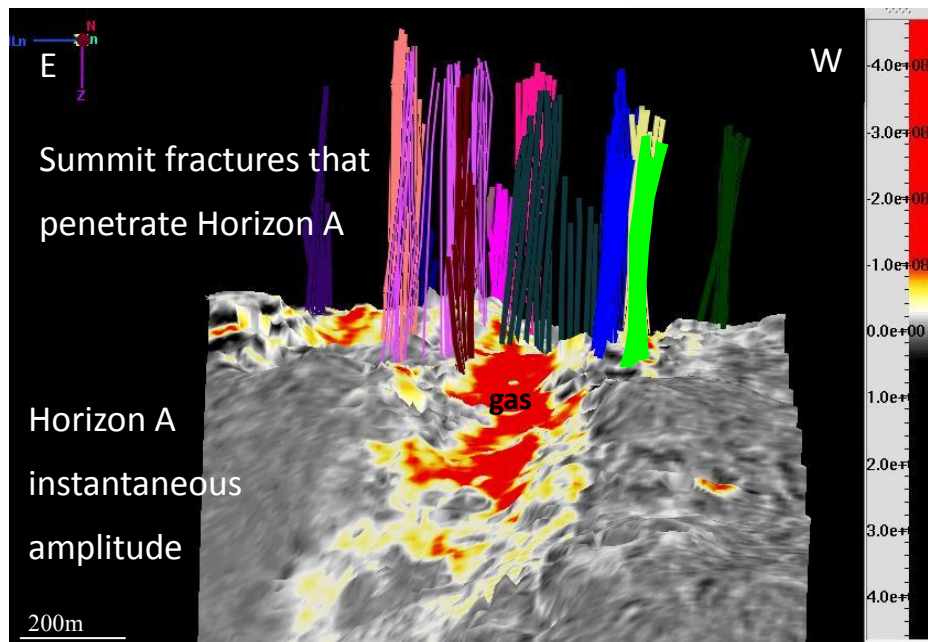


Figure 44: Perspective view looking up-dip of Horizon A (south). Fractures that penetrate Horizon A are shown with respect to Horizon A's instantaneous amplitude. The blue, lime green and pink fracture systems bound the bright amplitude zone where gas is assumed to be.

Bright, negative amplitudes are also present within Horizon A on the northern flank of the ridge, near the saddle of the north and south ridges (figure 27). The bright amplitudes are observed on the northern extent of our survey coverage, therefore it is not clear as to whether the anomalous amplitudes continue beyond the survey area to the north or not. These amplitudes coincide with the three deep cutting thrust faults on the northern flank (figure 35). There are no corresponding amplitude anomalies in the shallow section of these faults, suggesting that they are not supplying gas into the GHSZ. Instead, they may act as conduits for thermogenic methane to reach Horizon A, after which the gas migrates to the southern summit. A second explanation is that the gas may also be travelling along Horizon A from sources to the north of the three deep thrust faults.

Chapter 6: Summary

Interpretations of a new 3D high resolution reflection seismic volume improved constraints on the fluid migration system of south Hydrate Ridge, offshore Oregon. Hydrate Ridge is an active seafloor vent and gas hydrate environment, located roughly 60nm west of Newport, Oregon and the site of the ODP Leg 204 gas hydrate drilling initiative. This dynamic environment of active fluid flow and hydrate formation indicates a complex fluid migration network supplying gas through the hydrate stability zone to the seafloor. Previous research inferred that methane migrated into the GHSZ through an ash-rich turbidite layer, Horizon A, and primarily continued along lateral and stratigraphic conduits within the GHSZ. New insights from the high resolution 3D seismic volume indicate that the migration system is more complex than simple stratigraphic conduits. I propose that thermogenic methane travels within the ash-rich turbidite beds of Horizon A to the summit. At the summit, high gas saturations and pore-pressures initiate near-vertical fractures, through natural hydraulic fracturing of the weak sediments, to act as conduits to supply the gas to the seafloor vents. The fracture networks directly feed the seafloor vents from Horizon A and are independent from the laterally migrating methane within the GHSZ which feeds hydrate formation in porous stratigraphic units.

Horizon A is a coarse-grained, gas-saturated stratigraphic conduit composed of homogenous ash-rich turbidite beds, and therefore is an excellent conduit for methane. The bright, negative reflection amplitudes imaged in the new 3D seismic reflection survey indicate two regions of high gas saturation within Horizon A, one beneath the summit and the other on the northern flank. The composition of Horizon A and the continuity of the reflector suggest that it is a continuous, homogenous layer and

consequently the two gas accumulations are in communication with each other. The presence of the gas to the north, on the down-dip flank of Horizon A, suggests that the northern accumulation feeds the accumulation on the southern summit.

The new 3D survey interpretations indicate that networks of fractures formed beneath the summit of south Hydrate Ridge. They most likely formed as a result of hydraulic fracturing due to elevated free gas pressure exceeding hydrostatic pressure to the active fracture pressure of the weak sediments. These fractures provide permeable migration pathways within the hydrate stability zone, allowing for increased fluid flow and hydrate formation, as well as provide ample conduits for gas to migrate to seafloor vents. I believe that the formation of the fracture networks is controlled by the intermittent influx of deeply sourced thermogenic gas up in to the shallow 3D subsurface.

I observe in the seismic data ten near-vertical fractures within the gas hydrate stability zone (GHSZ) that do not extend beneath the BSR. I interpret these as remnant migration pathways that have subsequently filled with gas hydrate within the GHSZ and have sealed. The drop in internal pressures within the fractures as gases migrate along other pathways causes the segments below the GHSZ collapse from the surrounding high pressure while the segments that are hydrate-filled are physically maintained. Active conduits, such as the blue, lime, and magenta fractures depicted in figure 42, propagate from Horizon A to the seafloor and provide a direct migration pathway through the GHSZ. I speculate that over time, these too will become hydrate-filled and clog the upward flow of gas into the hydrate stability zone and into seafloor vents. Clogged fracture pathways will likely lead to additional gas accumulation and further build-up of gas pressure that may eventually lead to hydrofracture and development of new fractures. Thus, I conclude that the fluid migration of south Hydrate Ridge is a dynamic system

involving hydraulic fracturing driven by high gas pressures. From the interpreted data, I believe the methane gas influx drives the fracture network process at south Hydrate Ridge. This process occurring at south Hydrate Ridge supports those proposed to occur at Blake Ridge, offshore Vancouver Island and offshore Norway, where high gas pressures are thought to initiate fracture propagation within a gas hydrate environment (Flemings et al., 2003; Zühlsdoff and Spieß, 2004; and Hustoft et al., 2006).

The fractures develop and collapse as pore-pressures increase and decrease respectively. These fluctuations in pore-pressure could be driven by the buildup of free methane gas beneath the gas hydrate stability zone as fractures become hydrate-filled, rapid methane charging of the summit from the methane accumulation on the northern flank, or a combination of the two. I propose that high-energy tectonic events, such as earthquakes, trigger the release of the methane on the northern flank to the summit. Consequently, the sudden increase in gas saturation and pore-pressures could drive initial hydraulic fracturing through the sediments above into the GHSZ and the seafloor. The location of the authigenic pinnacle directly above the intersection of the BSR and Horizon A, the main gas supplier, indicates that this migration pathway was a long sustained one from Horizon A to the seafloor. Presumably, over time this conduit was hindered by gas hydrate forming within the fracture, shutting off methane transport to the seep and ultimately forming the authigenic pinnacle. Increased pore-pressures from the resulting gas accumulation could drive fracturing in other regions of the summit. There is no evidence to suggest locations of preferential fracturing, instead it appears that the fractures form at random within the zone above Horizon A's high gas saturations below the summit. These processes create a complex migration environment of intermittent methane transportation, hydraulic fracturing, seafloor venting, and gas hydrate formation.

References

- Bangs, N.L., Sawyer, D.S., and Golovchenko, X., 1993, Free gas at the base of the gas hydrate zone in the vicinity of the Chile triple junction: *Geology*, v. 21, p. 905-908.
- Chevallier, J., Tréhu, A.M., Bangs, N.L., Johnson, J.E., and Meyer, H.J., 2006, Seismic Sequence Stratigraphy and Tectonic Evolution of Southern Hydrate Ridge: *Proceedings of the Ocean Drilling Program, Scientific Results Volume 204*.
- Cochrane, G.R., Moore, J.C., MacKay, M.E., and Moore, G.F., 1994, Velocity and inferred porosity model of the Oregon accretionary prism from multichannel seismic reflection data: Implications on sediment dewatering and overpressure: *Journal of Geophysical Research*, v. 99, n. B4, p. 7033-7043.
- Collett, T., Kuuskraa, V., 1998, Hydrates contain vast store of world gas resources: *Oil and Gas Journal*, p. 90-95.
- Collett, T., 2002, Energy resource potential of natural gas hydrates: *AAPG Bulletin*, v. 86, p. 1971-1992.
- Collett, T., Riedel, M., Cochran, J., Boswell, R., Presley, J., Kumar, P., Sathe, A., Sethi, A., Lall, M., Sibal, V. and the NGHP Expedition 01 Scientists, 2006, *Indian National Gas Hydrate Program Expedition 01 Initial Reports*.
- Daigle, H. and Dugan, B., 2011, Capillary controls on methane hydrate distribution and fracturing in advective systems: *Geochemistry, Geophysics, Geosystems*, v. 12, Q01003.

- Daigle, H. and Dugan, B., 2010, Origin and evolution of fracture-hosted methane hydrate deposits: *Journal of Geophysical Research*, v. 115, B11103, p. 21.
- Davis, E. E., Becker, K., Wang, K., and Carson, B., 1995, Long-term observations of pressure and temperature in Hole 892B, Cascadia accretionary prism: *Proceedings of the Ocean Drilling Program, Scientific results*, v. 146, p. 299-311.
- Dev, A. and McMechan, G.A., 2010, Interpreting structural controls on hydrate and free-gas accumulation using well and seismic information from the Gulf of Mexico: *Geophysics*, v. 75, n.1, p. B35-B46.
- Flemings, P.B., Liu, X., and Winters, W.J., 2003, Critical pressure and multiphase flow in Blake Ridge gas hydrates: *Geological Society of America*, v. 31, n. 12, p. 1057-1060.
- Hedberg, H. D. 1979, Methane generation and petroleum migration: *Oil and Gas Journal*, May, p. 186-192.
- Heeschen, K.U., Tréhu, A.M., Collier, R.W., Suess, E., and Rehder, G., 2003, Distribution and height of methane bubble plumes on the Cascadia margin characterized by acoustic imaging: *Geophysics Research Letters*, v.30, p. 1643–1646.
- Henriet, J.P. and Mienert, J., 1998, Gas hydrates: the Gent debates. Outlook on research horizons and strategies: *Geological Society, London, Special Publications*, v. 137, p. 1-8.
- Hornbach, M. J., Saffer, D. M., and Holbrook, W.S., 2004, Critically pressured free-gas reservoirs below gas-hydrate provinces: *Nature*, v. 427, p. 142-144.

- Hubbert, M. K. and Willis, D.G.W., 1957, Mechanics of hydraulic fracturing: Trans. Am. Inst. Min. Eng., v. 210, p. 153-168.
- Hustoft, S., Mienert, J., Bünz, S., and Nouzé, H., 2007, High-resolution 3D-seismic data indicate focused fluid migration pathways above polygonal fault systems of the mid-Norwegian margin: Marine Geology, v. 245, p. 89-106.
- Hyndman, R. D. and Davis, E. E., 1992, A mechanism for the formation of methane hydrate and sea floor bottom-simulating reflectors by vertical fluid expulsion: Journal of Geophysical Research, v. 97, p. 7025-7041.
- Johnson, A., 2006, The role of gas hydrate in a global gas market: Gulf Coast Association of Geological Societies Transactions, v. 55, p. 373-381.
- Judd, A.G., 2003, The global importance and context of methane escape from the seabed: Geo-Mar Lett, v. 23, p. 147-154.
- Karaca, D., Hensen, C., and Wallmann, K., 2010, Controls on authigenic carbonate precipitation at cold seeps along the convergent margin off Costa Rica: Geochem. Geophys. Geosyst., v. 11.
- Korgen, B.J., Bodvarsson, G., and Mesecar, R.S., 1971, Heat flow through the flood of Cascadia Basin: Journal of Geophysical Research, v. 76, n. 20, p. 4758-4774.
- Kvenvolden, K.A., 1998, A primer on the geological occurrence of gas hydrate: Geological Society, London, Special Publications, v. 137, p. 9-30.
- Kvenvolden, K.A. and Lorenson, T.D., 2001, The global occurrence of natural gas hydrate: Natural Gas Hydrates: Occurrence, Distribution, and Detection, Geophysical Monograph 124, p. 3-18.

- Liu, X., and Flemings, P.B., 2006, Passing gas through the hydrate stability zone at southern Hydrate Ridge, offshore Oregon: *Earth and Planetary Science Letters*, v. 241, p. 211-226.
- Luo, X. and Vasseur, G., 2002, Natural hydraulic cracking: numerical model and sensitivity study: *Earth and Planetary Science Letters*, v. 201, p. 431-446.
- MacKay, M.E., Moore, G.F., Cochrane, G.R., Moore, J.C., and Kulm, L.D., 1992, Landward vergence and oblique structural trends in the Oregon margin accretionary prism: Implications and effect on fluid flow: *Earth and Planetary Science Letters*, v. 109, p. 477-491.
- MacKay, M.E., Jarrard, R.D., Westbrook, G.K., Hyndman, R.D. and Shipboard Scientific Party of Ocean Drilling Program Leg 146, 1994, Origin of bottom-simulating reflectors: Geophysical evidence from the Cascadia accretionary prism: *Geology*, v. 22, p. 459-462.
- Miller, J.L., Lee, M.L., and von Huene, R., 1991, An Analysis of a Seismic Reflection from the Base of a Gas Hydrate Zone, Offshore Peru: *The American Association of Petroleum Geologists Bulletin*, v. 75, p. 910-924.
- Milkov, A., Claypool, G.E., Lee, Y-J., Torres, M.E., Borowski, W.S., Tomaru, H., Sassen, R., Long, P.E., and ODP Leg 204 Scientific Party, 2004, Ethane enrichment and propane depletion in subsurface gases indicate gas hydrate occurrence in marine sediments at southern Hydrate Ridge offshore Oregon: *Organic Geochemistry*, v. 35, p. 1067-1080.
- Milkov, A. and Sassen, R., 2002, Economic geology of offshore gas hydrate accumulations and provinces: *Marine and Petroleum Geology*, v. 19, p. 1-11.

- Rao, Y. Subrahmanyam, C. and Sharma, S., 2001, Estimates of Geothermal gradients and Heat flow from BSRs along the Western Continental Margin of India: Geophysical Research Letters, no.2, p. 355-358.
- Shipley, T. Houston, M. Buffler, R. Shaub, F. McMillen, K. Ladd, J. and Worzel, J., 1979, Seismic evidence for widespread possible gas hydrate horizons on continental slopes and rises: American Association of Petroleum Geologists Bulletin, v.63, p 2204-2213.
- Singh, S.C., Minshull, T.A., and Spence, G.D., 1993, Velocity structure of a gas-hydrate reflector: Science, v. 260, p. 204-207.
- Sloan, E.D. Jr, 1998, Physical/chemical properties of gas hydrates and application to world margin stability and climate change: Geological Society, London, Special Publications, v. 137, p. 31-50.
- Suess, E., Torres, M.E., Bohrmann, G., Collier, R.W., Greinert, J., Linke, P., Rehder, G., Tréhu, A.M., Wallmann, K., Winckler, G., and Zuleger, E., 1999, Gas hydrate destabilization: enhanced dewatering, benthic material turnover and large methane plumes at the Cascadia convergent margin: Earth and Planetary Science Letters, v. 170, p. 1-15.
- Taylor, M.H., Dillon, W.P. and Pecher, I.A., 2000, Trapping and migration of methane associated with the gas hydrate stability zone at the Blake Ridge Diapir: new insights from seismic data: Marine Geology, v. 164, p. 79-89.
- Teichert, B.M.A. and Bohrmann, G., 2006, Data Report: Composition of Authigenic Carbonates in Sediments of the Cascadia Accretionary Prism, ODP Leg 204: Proceedings of the Ocean Drilling Program, Scientific Results Volume 204.

- Torres, M.E., Wallmann, K., Tréhu, A.M., Bohrmann, G., Borowski, W.S. and Tomaru, H., 2004, Gas hydrate growth, methane transport, and chloride enrichment at the southern summit of Hydrate Ridge, Cascadia margin off Oregon: *Earth and Planetary Science Letters*, v. 226, p. 225-241.
- Tréhu, A.M., Long, P.E., Torres, M.E., Bohrmann, G., Rack, F.R., Collett, T.S., Goldberg, D.S., Milkov, A.V., Riedel, M., Schultheiss, P., Bangs, N.L., Barr, S.R., Borowski, W.S., Claypool, G.E., Delwiche, M.E., Dickens, G.R., Gracia, E., Guerin, G., Hollard, M., Johnson, J.E., Lee, Y.-J., Liu, C.-S., Su, X., Teichert, B., Tomaru, H., Vanneste, M., Watanabe, M., and Weinberger, J.L., 2004a, Three-dimensional distribution of gas hydrate beneath southern Hydrate Ridge: constraints from ODP Leg 204: *Earth and Planetary Science Letters*, v. 222, p. 845-862.
- Tréhu, A.M., Flemings, P.B., Bangs, N.L., Chevallier, J., Gràcia, E., Johnson, J., Liu, C.-S., Liu, X., Riedel, M., and Torres, M., 2004b, Feeding methane vents and gas hydrate deposits at south Hydrate Ridge: *Geophysical Research Letters*, v. 31, L23310.
- Tréhu, A.M., Torres, M.E., Bohrmann, G., and Colwell, F.S., 2006, Leg 204 Synthesis: Gas Hydrate Distribution and Dynamics in the Central Cascadia Accretionary Complex: *Proceedings of the Ocean Drilling Program, Scientific Results Volume 204*.
- Tryon, M.D., Brown, K.M., Torres, M.E., Tréhu, A.M., McManus, J., and Collier, R.W., 1999, Measurements of transience and downward fluid flow near episodic methane gas vents, Hydrate Ridge, Cascadia: *Geology*, v. 27, n. 12, p. 1075-1078.

- Walsh, M., Hancock, S., Wilson, S., Patil, S., Moridis, G., Boswell, R., Collett, T., Koh, C., and Sloan, E, 2009, Preliminary report on the commercial viability of gas production from natural gas hydrates: *Energy Economics*, v. 31, p. 815-823.
- Zühlsdoff, L. and Spieß, V., 2004, Three-dimensional seismic characterization of a venting site reveals compelling indications of natural hydraulic fracturing: *Geology*, v. 32, n. 2, p. 101-104.

Vita

Emily Graham was born in 1987 in Windsor, England to parents Robert and Melise Graham. She graduated from Klein High School in Houston, TX in 2005 and attended the University of South Carolina in Columbia, SC. She graduated with honors in 2009 from the University of South Carolina with a Bachelor of Science degree in Geophysics. Emily then attended the University of Texas at Austin to pursue a Master of Science degree in Geological Sciences with the University of Texas Institute for Geophysics. Upon completion of her Master's degree in May of 2011, Emily will be working with Marathon Oil in Houston, TX as an Exploration Geophysicist on the Conventional New Ventures team in the Worldwide Exploration Group.

Permanent email: grahamem9@gmail.com

This thesis was typed by Emily Graham.